J. Space Weather Space Clim. 2024, **14**, 37
© V. Šimůnek et al., Published by EDP Sciences 2024
https://doi.org/10.1051/swsc/2024030

JSWSC
Available online at:
www.swsc-journal.org

Topical Issue – Space Climate: Long-term effects of solar variability on the Earth's environment

RESEARCH ARTICLE OPEN ACCESS

Norway spruce forest management in the Czech Republic is linked to the solar cycle under conditions of climate change – from tree rings to salvage harvesting

Václav Šimůnek[1,*], Zdeněk Vacek[1], Stanislav Vacek[1], Michal Švanda[2,3], Vojtěch Hájek[1], and Giuseppe D'Andrea[1]

[1] Czech University of Life Sciences Prague, Faculty of Forestry and Wood Sciences, Kamýcká 129, CZ – 165 21 Prague 6 – Suchdol, Czech Republic
[2] Astronomical Institute of the Czech Academy of Sciences, Fričova 298, 25165 Ondřejov, Czech Republic
[3] Astronomical Institute, Charles University, Faculty of Mathematics and Physics, V Holešovičkách 2, 18000 Praha, Czech Republic

Received 20 April 2023 / Accepted 13 September 2024

Abstract – Norway spruce (*Picea abies* [L.] Karst.) is the most important economic tree species in Central Europe. It has been affected by extensive windstorms and bark beetle disturbances, which have intensified in recent years. Spruce stands are subject to regular reoccurring disturbances with different intensities. This study examines timber harvests in the Czech Republic and the tree-ring series of Norway spruce from six permanent research plots across the country. The timber harvest shows a cyclical connection with the sunspot number, and of these, the percentage of spruce logging shows a substantial link with the sunspot number while the percentage of salvage logging indicates a relation with Total Solar Irradiance (TSI) and seasonal temperature. The seasonal North Atlantic Oscillation (NAO) indicated a link with logging types as well. However, the connection between TSI and SunSpot Number (SSN) with logging types was statistically significant, while the tree rings were more related to seasonal NAO than timber harvests. The tree Ring Width Index (RWI) series shows reduced growth, which precedes the peak in the timber harvests by 1 year. Timber harvests peak one year after minimum RWI, and they coincide with solar minimum years. In summary, average tree ring series reach predominantly their lowest values one year before the solar minimum, coinciding with increased spruce and salvage logging. Conversely, during the solar maximum, harvests are lower, and tree ring series remain relatively stable. In the spectral analysis, tree-ring series and all types of timber harvests show a quasi-11-year cycle. Spruce trees indicate higher tree-ring growth and lower timber harvests during solar maximum compared to solar minimum and this may be associated with specific meteorological conditions that may be affected by solar variability. European forestry is unfamiliar with the effects of the solar cycle; nevertheless, this phenomenon is present in both spruce tree rings and the aggregate of timber harvests. Further research on this issue will be necessary, but it is already apparent that regularly recurring calamities in spruce stands are likely to be reflected in all of Central Europe.

Keywords: Forest management / Sunspot number / Total solar irradiance / *Picea abies (L.) Karst. / North Atlantic Oscillation*

1 Introduction

The forests of Central Europe – Norway spruce (*Picea abies* [L.] Karst.), in particular – are crucially affected by climate change. Forest management of this most widespread tree species, on which Czech forestry economically depends, is expected to face increasing difficulties (Thiele et al., 2017). Spruce stands have suffered large-scale damage during the recent years of climate change (MAF, 2018; Toth et al., 2020). Europe is challenged by more frequent wildfires or intense windthrow with uneven distribution of precipitation and increasing temperatures caused by climate change (Kundzewicz et al., 2006; Vacek et al., 2023). Climate change has also influenced coniferous tree silviculture in the Czech Republic and neighboring countries, which have recently experienced damage from periodic droughts (Ashraf et al., 2015; Alvarez et al., 2016; Noce et al., 2016; Tumajer et al., 2017). Spruce stands account for the largest tree species representing, 49.5% in the Czech Republic. The entire

*Corresponding author: simunekv@fld.czu.cz

forestry sector is based on coniferous tree production, while 71% are coniferous stands, the rest (29%) are deciduous stands (MAF, 2020). Norway spruce is one of the coniferous species less adaptable to drought during the summer months due to its poor ability to reach moisture deeper in the soil profile (Hartl-Meier et al., 2018).

The poor condition of spruce stands is also accompanied by outbreaks of bark beetle infestation, reoccurring predominately in dry years and thus, enhancing the disintegration of spruce stands (Kopáček et al., 2015; Nováková & Edwards-Jonášová, 2015). More frequent logging operations lead to infestations with other secondary pests, such as fungal diseases *Heterobasidion* spp. and *Armillaria* spp. (Aosaar et al., 2020; Blomquist et al., 2020). One of the common fungal diseases, *Heterobasidion annosum* (Fr.) Bref., weakens the base of spruce trunks, making them more susceptible to breakage and overturning (Piri, 1996; Vacek et al., 2020). The health status of spruce is also complicated by the disease of the root system, *Armillaria* spp., which weakens spruce stands during drought, increasing their susceptibility to bark beetle attacks (Holuša et al., 2018). As a result of climate change, dieback has led to the decline of spruce stands in recent years (Čermák et al., 2019). Game browsing and bark stripping further undermine the health of forest stands, making them more sensitive to climatic factors, especially drought, which reduces the increment and stability of spruce stands (Cukor et al., 2019; Krisans et al., 2020).

Stimulated by the climate, populations of *Ips typographus* (L.) and other bark beetles increase and attack healthy trees as well (Marini et al., 2017; Netherer et al., 2019). The general decline of spruce in the Czech Republic is compounded by the overall aging of forest stands: the amount of stands over 81 years of age is progressively increasing which can be seen in the report from 2021, along with the amount of salvage logging, even in the older forests (MAF, 2021). Old spruce stands, in particular, are more sensitive to temperature fluctuations (Kukumägi et al., 2017; Vacek et al., 2019). Older spruce forests are sensitive to higher temperatures due to their reduced ability to adapt to climate changes, resulting in excessive drought and subsequently increasing tree vulnerability to pests such as bark beetles (Hlásny et al., 2017). In addition, the older the forest stand, the higher the risk of disturbance (Vacchiano et al., 2013) and of *Ips typographus* that primarily attacks weakened trees older than 60 years (Schroeder & Lindelöw, 2002; Hlásny & Turčáni, 2013).

Climate change has proven to have a negative impact on forestry economic indicators affecting spruce management, which ostensibly fails to eliminate negative climate variability (Hlásny et al., 2017). Higher short-term salvage logging, induced by ecological calamities, lowers timber prices, which directly impacts forest management (Remeš et al., 2020; Toth et al., 2020). All impacts combined reduce the economic value of forests in the long term (Hanewinkel et al., 2013) and potentially challenge atmospheric carbon fixation as well (Dobor et al., 2020). Climatic fluctuations force forest management to adapt silviculture to nature's unexpected changes (Spiecker, 2003).

The periodic influence of the 11-year solar cycle on climate may offer a partial answer to the cyclical disintegration of forests. The 11-year cycle is observed in the forest environment and tree rings (Matveev et al., 2017; Komitov, 2021). Sunspot cycles have been observed to influence many factors such as the ozone layer, stratospheric temperature, El Niño-Southern Oscillation, zonal winds, etc. (Rigozo et al., 2007; Maycock et al., 2016, 2018; Ball et al., 2019; Tartaglione et al., 2020). Solar activity can influence the temperature and precipitation extremes of the Earth's atmosphere, e.g., during colder winter periods or during the summer European weather patterns (Gray et al., 2010; Rimbu et al., 2021).

The solar activity cycle also manifests in total solar irradiance, which causes the TSI fluctuations of 0.1% (Kopp et al., 2016). A direct connection is assumed between the 11-year solar cycle and temperatures in specific geographic regions during certain multi-decadal periods, specifically in February, March, June, and September (Lüdecke et al., 2020) and indirectly, also with the North Atlantic Oscillation (NAO) and the Atlantic Multidecadal Oscillation (AMO) – (Bice et al., 2012). Jet streams exhibit non-uniformity in terms of wind speed and altitude along their length, often featuring fragmented sections with the greatest baroclinicity. The variability and mean flow tend to maximize over oceanic regions (Blackmon, 1976). Recent studies have presented conflicting results regarding the solar cycle influences on winter climate over the North Atlantic/European region. Polar front jet stream variability is responsible for instances of extreme weather and is crucial for regional climate change, particularly affecting western Europe and eastern North America (Brugnara et al., 2013; Hall et al., 2015; Ma et al., 2018). The modulation effect of solar variability on the North Atlantic Oscillation (NAO) is currently a topic of controversy. In recent discussions, arguments both in favor (Drews et al., 2022) of and against (Chiodo et al., 2019; Spiegl et al., 2023) the solar impact on NAO have been analyzed.

The Quasi-Biennial Oscillation (QBO) is a repeating wind pattern in the Earth's stratosphere that changes direction approximately every 28–29 months. During the QBO's east phase, there is an increased likelihood of sudden stratospheric warming, leading to a warm polar stratosphere and potential cooling over Northern Europe. Observations show a positive correlation between 30-hPa North Pole troposphere temperatures and the 11-year solar cycle during the QBO's west phase, while no correlation is observed during its east phase. Observations indicate an enhanced likelihood of sudden stratospheric warming during the QBO east phase, leading to a warming of the polar stratosphere and potentially causing cooling over Northern Europe in the troposphere by triggering cold air outbreaks (Labitzke, 2005). This short-term 28-month cycle significantly influences stratospheric and tropospheric temperatures (Baldwin et al., 2001; Coy et al., 2017). The circulation over Europe is also linked with El Niño-Southern Oscillation (ENSO) which affects weather patterns worldwide. It involves the periodic warming (El Niño) and cooling (La Niña) of sea surface temperatures in the central and eastern tropical Pacific Ocean. In Europe, it can influence winter weather by altering the position and strength of the jet stream, leading to shifts in atmospheric pressure patterns. El Niño is associated with milder and wetter conditions, while La Niña tends to bring colder and drier weather. These ENSO-related changes can impact European regions, affecting precipitation, temperature, and even extreme events (Brönnimann, 2007; Cai et al., 2010). Variations in the cloud cover show similarities with the variability modes of the ENSO, NAO, and QBO. Several publications highlight a solar influence on the summer monsoon, primarily through variations in TSI. For instance, studies have shown that changes in

TSI can impact the Asian summer monsoon, affecting weather patterns (Wang et al., 2005; Shi et al., 2014).

The European climate is significantly impacted by the NAO and shifting wind patterns, which respond differently to climate change along latitude gradients. The NAO has a modest early-season influence on summer temperatures (Kjellström et al., 2013) and affects both precipitation and airflow patterns during dry seasons (Tsanis and Tapoglou, 2019). The NAO has positive and negative phases. A negative phase can bring cooler, drier conditions to Central Europe, while the positive phase does the almost opposite (Vicente-Serrano et al., 2011; Yao & Luo, 2014; Steirou et al., 2017; Tatli & Menteş, 2019).

The NAO and solar cycle dynamics also manifest in annual tree growth. While NAO-tree ring responses vary across Europe, they are often tied to local climate and seasonal growth effects. Central Europe has witnessed changing NAO-related tree-ring responses over the past century, with distinct trends in the 20th century compared to the 19th century (St. George, 2014). Notably, during February, NAO can indirectly impact tree-ring growth by influencing precipitation and groundwater levels (Akhmetzyanov et al., 2023).

Various dendrochronological research studies also demonstrated the influence of solar cycles on the radial growth of different tree species, in studies from Northwest Russia (Shumilov et al., 2011; Kasatkina et al., 2019), Chile (Rigozo et al., 2002), the Tibetan Plateau (Wang & Zhang, 2011), or Central and Southern Europe (Surový et al., 2008; Šimůnek et al., 2021b). The effect of the solar cycle on the growth of trees has been observed in the annual rings of trees in the past. The fossil finds revealed the presence of an 11–15-year cycle in tree-rings data in central Italy (Cecchini et al., 1996). There are also studies describing the coincidence of solar cycles with forest fire risk (Uğur & Feriha, 2017). Studying climate patterns like the North NAO and solar cycle can enhance our understanding of mechanisms. This knowledge, coupled with insights into the cyclic processes, has the potential to significantly aid forestry and timber-processing management in adapting to these fluctuations through enhanced prediction. Forest management planning and ecological stability of the stands will benefit from the knowledge of forest calamity cycles, which will also result in reduced economic losses.

This study aims to compare the radial growth of spruce with harvesting and the course of the solar cycle. It describes the tree-ring growth of Norway spruce at different plots in the Czech Republic, types of forest timber harvests for the entire Czech Republic, and data for total, salvage, and spruce harvests. Two time periods were evaluated: 1900–2019 and 1961–2019. Tree-ring growth of Norway spruce and different types of timber harvest in the Czech Republic were compared with the sunspot number, total solar irradiance, air temperature, seasonal temperature, precipitation, seasonal precipitation, annual NAO, and seasonal NAO. The datasets used in this study describe the relationship in the oscillations between timber harvests and tree-ring series with respect to the course of precipitation, temperatures, NAO, total solar irradiance, and the sunspot cycle. An important objective of this study is not only to demonstrate the climatic influences affecting timber harvesting and tree-ring series but to also understand the sequence and order of factors preceding fluctuations in salvage logging and spruce timber harvests. The influence of the 11-year cycle on the development of timber harvesting and ring-width index has not been jointly compared so far. Therefore, with this study, we hope to generate a new perspective on the relative roles of the various influencing factors and the involved process in forest calamities in central Europe and their possible connection with tree rings and climate data fluctuations.

2 Methodology

2.1 Study area

The study area for the dendrochronological analysis is located in the Czech Republic. The research plots are situated according to altitude and occupy lower-lying, middle, and mountain positions. A total of six research plots were evaluated, of which the first two – the Karlštejn (1_KAR) and Kostelec (2_KOS) plots – belong to the lower positions, while the Jeseník (3_JES) and Podkrkonoší (4_POD) plots are mid-altitude positions, and Orlické hory (5_ORL) and Bažinky (6_BAZ) plots classify as mountain sites. Dendrochronological samples from these plots were obtained from forest stands with dominant Norway spruce. The research plots of 6_BAZ, 3_JES, and 5_ORL are located in the no-logging areas, where no logging operations have been conducted since 1985, and prior to that, a shelterwood system based on selection logging had been applied. In contrast, the research plots of 4_POD, 1_KAR, and 2_KOS are commercial forest stands managed in close-to-nature ways based on a shelterwood system, target trees, and the tending of the growing stock. Trophic and mesotrophic cryptopodzols to nutrient-poor, oligotrophic soils of gleys and podzols dominate on the surveyed sites. Soil moisture conditions in the study plots range from dry to gleyed soils. Table 1 provides more information on the individual research plots.

The precipitation and air temperature conditions vary across the Czech Republic, therefore, meteorological stations nearest to the research plots were used for the dendrochronological analyses (Fig. 1a). The basic habitat and stand characteristics of the plots are given in Table 1. In the Czech Republic, lower altitudes are primarily influenced by the continental climate: according to Koppen's classification (Köppen, 1936), the lower altitude sites are in the climatic region Cfb – temperate oceanic climate with warm summer without dry seasons. The middle elevations fall within region Dfb – a warm-summer humid continental climate characterized by hot summers and cold winters. The higher elevations are region Dfc – subarctic cold (continental) climate with cold summers without a dry season (Köppen, 1936). The annual air temperature in the Czech Republic ranges from +9.5 to −0.4 °C, with an average of 7.9 °C, and the annual precipitation ranges from 410 to 1705 mm with an average of 650 mm for the entire country in relation to altitude, from 115 to 1603 m a.s.l. The average altitude in the Czech Republic is 430 m a.s.l. The lowest average air temperature in January is −2.0 °C, and the highest average air temperature in June is 17.8 °C (ČHMÚ, 2022).

2.1.1 *Demographic evolution of the forests in the Czech Republic*

Forest ecosystems in the Czech Republic have undergone significant transformations from 1900 to the present. Following

Table 1. Basic plot and stand characteristics of Norway spruce research plots in 2019.

Plot name	Plot ID	Location	Altitude (m a.s.l.)	Exposure	Slope (%)	Mean height (m)	Mean DBH (cm)	Volume ($m^3 \cdot ha^{-1}$)	Forest type	Temp. (°C)	Prec. (mm)	Climate classif.
1_KAR	1	49°56′26.8″N 14°12′05.6″E	420	NW	5	25	34	520	3B1	8.63	539	Cfb
2_KOS	2	49°58′33.5″N 14°47′20.9″E	425	NE	10	30	35	685	3I1	7.92	670	Cfb
3_JES	3	49°56′57.3″N 17°13′81.7″E	670	SE	4	24	32	398	5O1	6.35	694	Dfb
4_POD	4	50°37′34.9″N 15°46′30.2″E	670	SW	18	38	35	598	5S1	7.31	742	Dfb
5_ORL	5	50°22′44.4″N 16°21′36.4″E	800	SW	8	23	28	364	6K1	6.41	1087	Dfb
6_BAZ	6	50°44′0.6″N 15°32′7.3″E	1020	E	22	30	52	498	7S1	5.06	1333	Dfc

Notes: NW – northwest; NE – northeast; E – east; SE – southeast; 7S1 – *Fageto-Piceetum oligomesotrophicum*; 5S1 – *Abieto-Fagetum mesotrophicum, Avenella flexuosa*; 3B1 – *Querceto-Fagetum mesotrophicum, Melica uniflora*; 3I1 – *Querceto-Fagetum illimerosum acidophilum, Luzula pilosa*; 5O1 – *Fageto-Abietum variohumidum mesotrophicum, Oxalis acetosella*; 6K1 – *Piceeto-Fagetum acidophilum, Calamagrostis villosa* (Viewegh et al., 2003); DBH – average diameter at breast height; Temp. – mean year air temperature; Prec. – annual precipitation; Climate classification according to Köppen (Köppen, 1936): Cfb – temperate oceanic climate; Dfb – warm-summer humid continental climate; Dfc – subarctic climate.

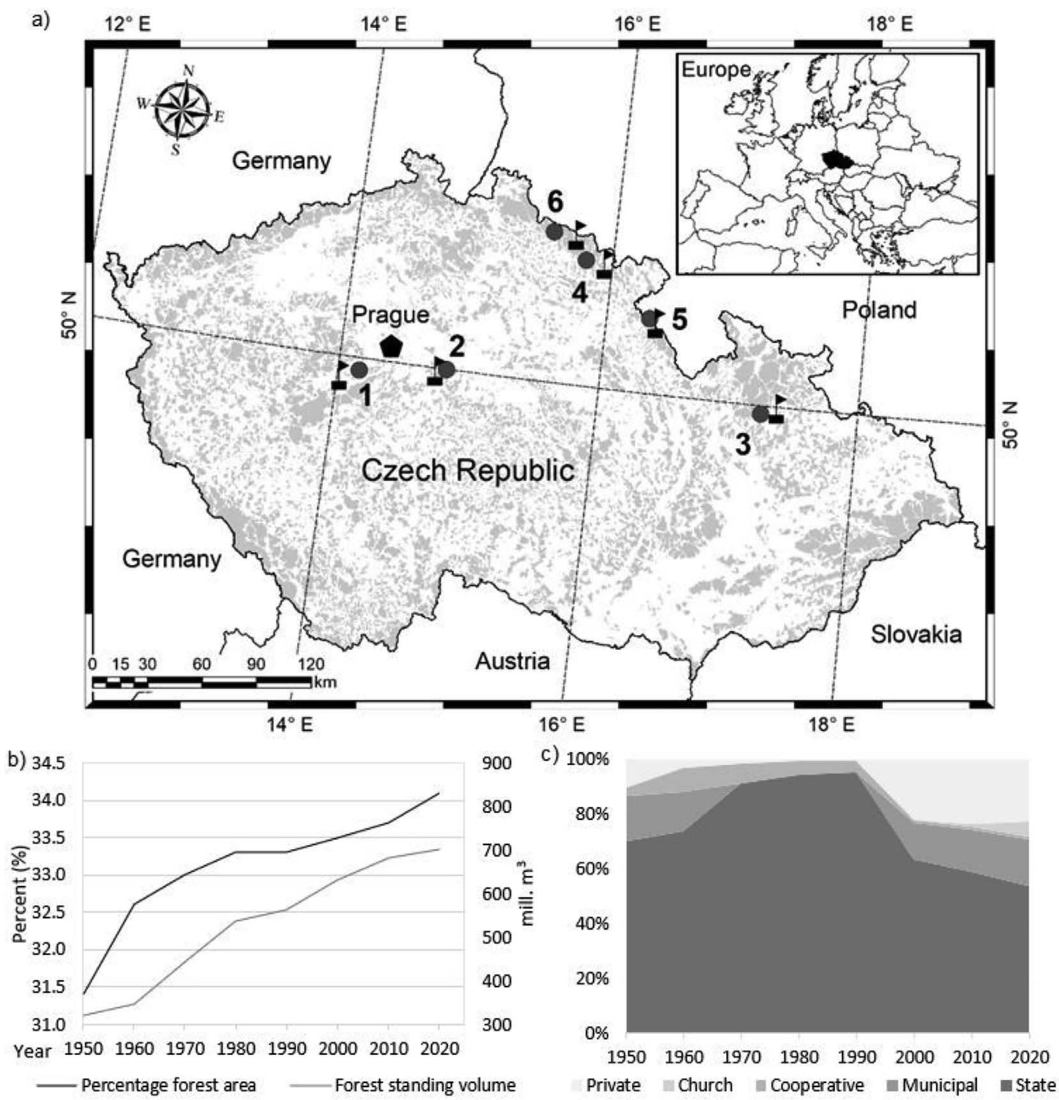

Figure 1. Location of research plots 1–6 (grey dots) and the meteorological stations used for dendrochronological analyses (black flags); the grey pentagon indicates the capital city Prague (upper map). Research plots number: 1–1_KAR; 2–2_KOS; 3–3_JES; 4–4_POD; 5–5_ORL; 6–6_BAZ (a). The change of the fraction of forest area and total volume of forest stands (b) as well as forest ownership (c) in the Czech Republic in ten-year intervals from 1950 to 2020.

the aftermath of the First World War, the forest cover declined to approximately 30%. However, subsequent efforts in afforestation on previously unused lands resulted in an increase in forest cover to around 34% by 2020 (Fig. 1b). The most extensive afforestation took place after the Second World War when privately owned lands were nationalized and converted into state forests. Another significant event affecting forestry was the air pollution catastrophe from high concentrations of SO_2 in the mountainous regions of the Czech Republic during the seventies and eighties, particularly in the mountain ranges bordering Germany and Poland (Materna, 1989; Vacek et al., 2015a).

The political regime changes in 1992 resulted in the transformation of state forests into private ownership (as depicted in Fig. 1c). Since the 1990s, the existing forest stands have gradually aged, accompanied by an increased adoption of mechanization in forest management practices. This mechanization trend has led to a reduction in the number of forestry employees from 70,000 in 1985 to 14,000 in 2020 (CZSO, 2021). The reduction in the number of employees led to insufficiently fast processing of bark beetle-infested wood, allowing the calamities to grow to larger proportions, subsequently exerting pressure on the price of bark beetle-infested wood (Hlásny et al., 2021a). The situation after the restitution (return) of forest stands to private ownership in the 1990s also resulted in the fragmentation of smaller land properties, which in many cases led to an increase in bark beetles and delays in the processing of infested wood, a situation that continues to persist until today (Seidl et al., 2016).

Since the year 2000, there has been a notable increase in forest stand mortality, primarily affecting Norway spruce and other coniferous species. Climate change is considered the main driver behind this calamity, with higher average temperatures and inadequate precipitation during critical climatic periods. These unfavorable conditions have contributed to the bark beetle graduation calamities which are the most significant secondary problem after the drought of the current Czech forestry (MAF, 2021).

2.2 Data collection

For the dendrochronological analysis of the samples, increment cores were taken from Norway spruce using a Pressler auger (Haglöf, Långsele, Västernorrland, Sweden) perpendicular to the trunk axis at a height of 1.3 m above the ground. Structurally homogeneous spruce stands with a stand density of 0.8 (80%) to 1 (100%) were selected for sampling. Samples were collected from square 50 × 50 m study plots from healthy co-dominant and dominant trees compared to sub-dominant and suppressed trees (Remeš et al., 2015) with an average diameter at breast height (DBH) > 25 cm. Height was measured with a Laser Vertex hypsometer (Haglöf, Långsele, Västernorrland, Sweden) to an accuracy of 0.1 m for all trees with increment cores obtained. For all trees, the DBH was also measured with a Mantax Blue metal caliper (Haglöf, Långsele, Västernorrland, Sweden) with a precision of 1 mm. A total of 318 samples were collected for dendrochronological analysis, with sample core numbers per plot ranging from 40 to 58 per plot (Table 3). The cores were measured using a LINTAB measuring stage with an Olympus microscope. The measuring table gauges to an accuracy of 0.01 mm, and TSAP-Win software (Rinntech, 2010) was used to record the increment cores. Subsequent cross-dating of the core samples was performed in the CDendro program (Cybis Elektronik & Data AB, Sweden) so that the cross-correlation index was CC > 25 for each sample (Larsson, 2013).

Monthly temperature and precipitation data for the whole Czech Republic were provided and statistically prepared by the Czech Hydrometeorological Institute, Prague[1]. This study also used data from the longest measuring climatic station in the Czech Republic, Klementinum (altitude 191 m a.s.l.; 50°5′12″N, 14°24′56″E). The vegetation season extends from May to September. A detailed overview of the meteorological stations used and their relationship to the research plots is shown in Table 2.

The annual mean sunspot number data were provided by the Royal Observatory of Belgium, Brussels[2]. Data on the annual TSI were taken from the composite of the TSI measurements and reconstruction by Greg Kopp running up to the year 2019 (Dudok de Wit et al., 2017). Additionally, for the period prior to 1978, the TSI reconstruction by Wu et al. (2018) using the SATIRE model was incorporated. The TSI reconstruction was made available by G. Kopp on his webpage[3]. The TSI model is composed of a total irradiance model that captures 92% variance of sunspot number and absolute scale creation is reported and explained by Kopp & Lean (2011).

Timber harvest data were obtained from the Forest Management Institute in Brandýs nad Labem, Czech Republic[4] and the Czech Statistical Office in Prague, Czech Republic[5]. The total harvested timber is the volume of large timber (apart from logging residues), including self-production (self-production refers to wood collection by individuals, either partially or entirely, in exchange for a predetermined fee or without any charge). Timber from logging and silvicultural operations includes salvage logging. The total coniferous timber logging in the Czech Republic also includes salvage logging in coniferous stands. The total spruce timber logging in the Czech Republic includes salvage logging too. Salvage logging data cover all types of salvage logging and calamities caused by abiotic and biotic factors. It also includes dead-standing trees, isolated breaks, uprootings, all of the trees felled for trapping bark beetles, and individual trees in which harmful insects (bark beetles, etc.) spend the winter (Nownes, 2012).

To eliminate political and economic influences on timber harvesting, salvage logging, and spruce logging have been converted into percentage shares of the main harvests. This step eliminates quantity fluctuations in timber harvesting dependent on economic planning and better captures overall fluctuations in these types of logging. Since salvage logging is a practical forestry operation carried out as quickly as possible to assess the damage, it is possible to say that climatic fluctuations best

[1] Czech Hydrometeorological Institute of the Czech Republic (CHMI) https://www.chmi.cz/ (accessed 2022-10-01).

[2] Royal Observatory of Belgium (WDC-SILSO) https://www.sidc.be/silso/ (accessed 2022/12/10).

[3] Greg Kopp TSI data at https://spot.colorado.edu/~koppg/TSI/ (accessed 2021/02/04).

[4] Forest Management Institute (ÚHÚL) in Brandýs nad Labem at https://www.uhul.cz/portfolio/poskytovani-dat/ (accessed 2022/10/01).

[5] Czech Statistical Office (CZSO) in Prague at https://www.czso.cz/ (accessed 2022/10/01).

Table 2. Location and meteorological characteristics of Norway spruce research plots in 2019.

Plot name	Meteorological station name	GPS of Meteorological station	Meteorological station altitude (m a.s.l.)	Distance to research plot (km)	Vegetation season period (month range)
1_KAR	Neumětely	49°51′00″N 14°02′24″E	322	25	May–September
2_KOS	Ondřejov	49°54′36″N 14°46′48″E	485	7	May–September
3_JES	Světlá Hora	50°02′46″N 17°23′50″E	593	16.6	May–August
4_POD	Trutnov	50°34′10″N 15°54′42″E	460	11.5	May–September
5_ORL	Deštné v Orlických horách	50°18′22″N 16°21′04″E	656	8.1	May–September
6_BAZ	Pec pod Sněžkou	50°41′30″N 15°43′43″E	816	14.4	May–August

Table 3. Characteristics of tree-ring chronologies for Norway spruce in research plots for time period 1900–2019.

Plot name	No. trees	Mean RW (mm)	SD RW	Mean min – max (mm)	Age min – max	ar1	R-bar	EPS	SNR
1_KAR	57	1.69	0.92	0.99–2.58	54–92	0.60	0.54	0.98	54.22
2_KOS	58	1.84	0.82	1.03–3.34	29–136	0.69	0.42	0.97	31.43
3_JES	57	3.01	1.23	1.15–5.97	34–132	0.76	0.27	0.91	10.54
4_POD	48	2.36	1.18	1.34–3.59	71–112	0.77	0.23	0.92	11.17
5_ORL	40	2.29	1.09	0.88–4.20	37–160	0.80	0.32	0.90	8.87
6_BAZ	58	1.69	0.89	1.03–3.38	81–240	0.83	0.46	0.98	38.95

Notes: No. trees – number of trees; Mean RW – mean ring width in mm; SD RW – standard deviation from ring width in mm; Mean min–max – mean ring width range in mm from smallest to biggest tree; Age min–max – age range of youngest and oldest sample tree; ar1 – first order autocorrelation; R-ar – inter–series correlation; EPS – expressed population signal; SNR – signal to noise ratio.

mirror the development of salvage logging to weather fluctuations, bark beetle damage, and other pests. Given that conifers are known to be more sensitive to climatic fluctuations and sudden events, spruce, which is also the most represented conifer species in the Czech Republic, is most harvested during salvage logging.

The data on the NAO are obtained from the webpage of the Climatic Research Unit, University of East Anglia[6]. The data of the annual and monthly NAO index are derived from Gibraltar and South-west Iceland. During the winter season, the contrast between the standardized sea level pressure in Gibraltar and Southwest Iceland serves as a valuable indicator of the NAO intensity (Jones et al., 1997; CRU-UEA, 2023).

Figure 2 shows the main data used for different types of logging, sunspot number, TSI, precipitation, temperature, and NAO in this study (climatic data from the meteorological stations are not shown due to the extensive amount of data).

2.3 Data analysis

Dendrochronological data for Norway spruce (the data are described in result Sects. 3.1 and 3.2) were processed with the R software (Team R Core, 2022) using the "dplR" package (Bunn, 2008; Zang et al., 2018). Detrending of each tree was performed by the "dplR" package (Bunn, 2008, 2010). A two-step negative exponential detrending with spline (of n = 67% of series length) was used on each tree. Detrending removes the age trend while preserving low-frequency climate signals (Cook et al., 1990; Shumilov et al., 2011). The detrended tree-ring growth data are denoted as tree ring-width index (RWI) further. The expressed population signal (EPS) was calculated for the detrended data. The EPS serves as a metric for assessing the reliability of a chronology and is determined by a combination of inter-series correlations R-bar and sample size (Fritts, 1966; Anthony et al., 2003). The EPS represents the reliability of a chronology as a fraction of the joint variance of the theoretical infinite tree population. The limit for using the data for comparison against climate data was a significant EPS threshold, EPS > 0.85 (Bunn et al., 2018). Also, the signal-to-noise ratio (SNR) was calculated, which represents the signal strength of chronology, and inter-series correlations (R-bar). The SNR is a statistical measure that compares the strength of the desired signal in a data set of series to the level of background noise. A higher value of SNR represents a stronger climatic signal relative to noise. The R-bar describes the similarity of tree-ring patterns across multiple samples. R-bar is the average pairwise correlation coefficient between individual trees within a chronology. A higher R-bar value indicates stronger coherence among the tree-ring patterns (Fritts, 1976). The first-order autocorrelation (ar1) was also calculated. The ar1 refers to the degree of correlation between a data point and the preceding one in a time series of tree ring chronology. The EPS, SNR, R-bar, and ar1 indexes were calculated according to the instructions in the "dplR" (Bunn et al., 2018) and are based on general dendrochronological theories (Fritts, 1976; Speer, 2010).

Table 3 shows basic descriptive data obtained for the research plots from which tree-ring analyses were conducted to describe tree-ring spruce series measured (LINTAB). These indicators in the table are calculated for the period from 1900 to 2019 that is used in the study. Data for this table was acquired using the dendrochronological method described in Section 2.2. The table clearly presents the course of mean ring width (RW) and mean min–max (mm), which was derived from undetrended tree-ring curves. The indicators ar1, R-bar, EPS, and SNR of the detrended tree-ring series are used in our results.

[6] Climatic Research Unit, University of East Anglia at https://crudata.uea.ac.uk/cru/data/nao/ (accessed 2023/9/15).

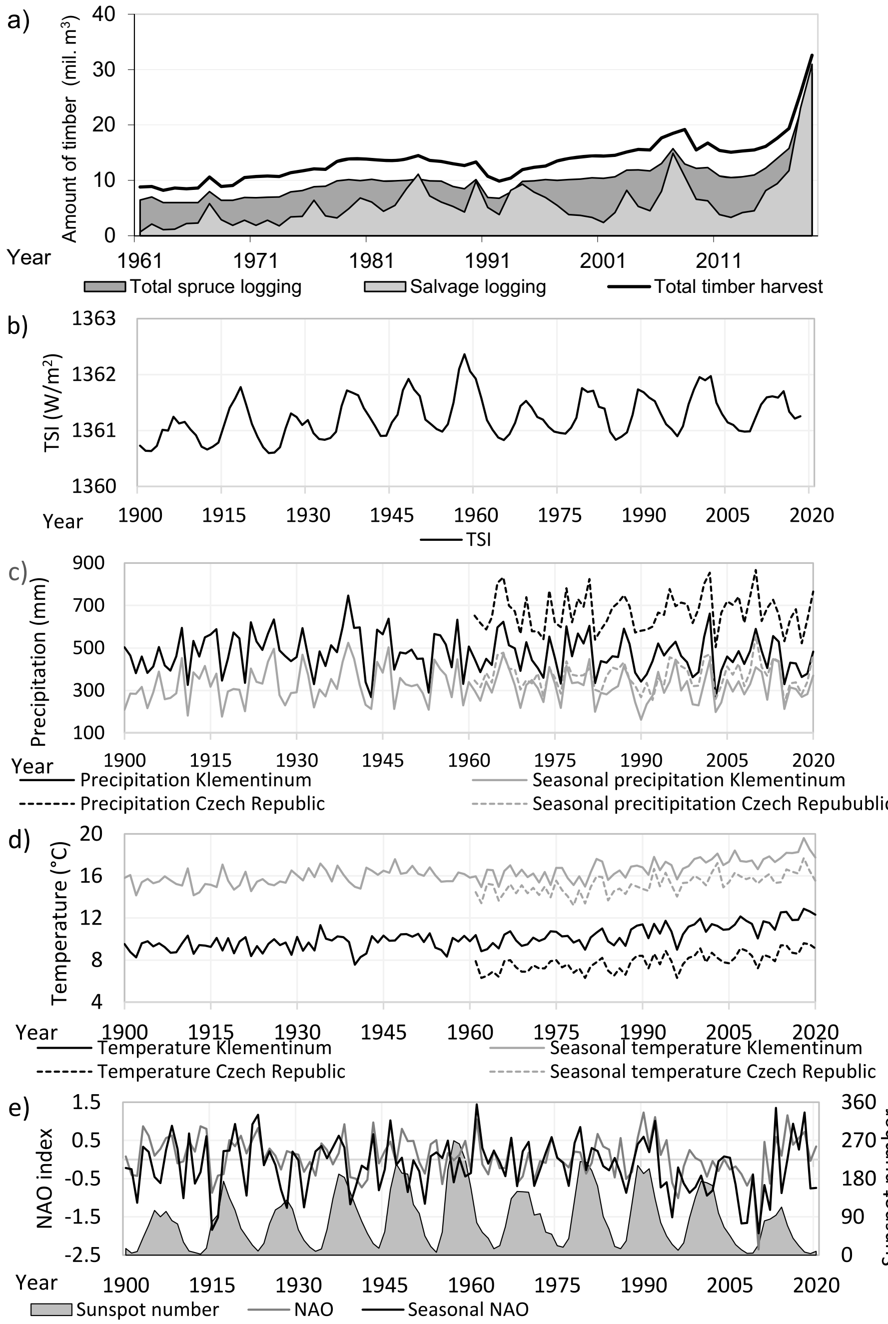

Figure 2. Open access or institutional data used in this study: (a) Dynamics of total timber harvest, total spruce timber logging, and salvage logging in the Czech Republic, the amount of timber in mill. m^3 – million cubic meters of harvested timber; (b) Total solar irradiance (TSI); (c) Precipitation from the longest monitored meteorological station, Klementinum (1900–2019), and from the Czech Republic (in 1961–2019); (d) Air temperature from the Czech Republic (in 1961–2019) and from the longest measuring meteorological station, Klementinum (1900–2019); (e) North Atlantic Oscillation and sunspot number.

To investigate the influence of sunspot number and TSI on tree-ring growth and timber harvesting, all data were analysed. Precipitation, temperature, and NAO data were also evaluated in relation to tree ring growth, as they play a crucial role in the forest environment. In addition, cyclical or causal order relationships were described using spectral analysis, and superposed epoch analysis (SEA) on the main tree ring data and types of timber harvesting. Furthermore, the cyclical relationships between timber harvesting and tree ring series were investigated, which could potentially explain their mutual relationship in comparison to solar activity.

Spectral analyses of the data were performed with the Statistica 13 software (StatSoft, 2013). The calculation was performed with the "Single Fourier (Spectral) Analysis" function, using the output of the "Periodogram" plot by "Period." The periodogram values are interpreted in terms of variance (sums of squares) of the data at the respective period. The periodogram ascribes values to periods. Additionally, multiple linear regression analyses were calculated using this software.

The statistical analysis, conducted with the Statistica software (StatSoft, Tulsa, CA, USA), a multiple linear regression approach was employed to explore the relationships between various independent variables and the dependent variable. The Multiple R field shows the coefficient of multiple correlation, representing the positive square root of R-square (the coefficient of multiple determination). This statistic is handy in multivariate regression, particularly when dealing with multiple independent variables, to describe the relationship between these variables. An overall F-test (F) was performed to assess the association between the dependent variable and the set of independent variables, with the F-value and its corresponding p-value serving as crucial indicators (F = Regression Mean Square/Residual Mean Square). The overall F-test is founded on the null hypothesis that all coefficients are zero. Therefore, it serves to identify models that are clearly mis-specified, although it is not designed to quantify how good a model is. In multiple linear regression, it is typically assumed that the residuals (observed minus predicted values) follow a normal distribution. While F is generally robust even if this assumption is violated, it is prudent to review the distributions of the main variable of interest before reaching final conclusions. F is used to show relationships between the dependent variable and the set of independent variables. Additionally, an Adjusted R^2 value was computed, akin to the R^2 coefficient, but adjusted to account for the degrees of freedom by considering the error sum of squares and total sums of squares. The df is degrees of freedom (different in the numerator and denominator) while "Residual S2" is the error sums of squares and the "Total S2" is the total sums of squares. The R^2 Adjusted is described by equation:

$$R^2\text{Adjusted} = 1 - [(\text{Residual S2}/\text{df})/(\text{Total S2}/\text{df})].$$

The results are presented as standardized (b^*) and non-standardized (b) regression coefficients along with their standard errors and statistical significance. The b^* coefficients offer insights into the relative contributions of each independent variable when all variables are standardized to a mean of 0 and a standard deviation of 1, aiding in the prediction of the dependent variable (StatSoft, 2013). The first multiple linear regression used the dependent percentage of salvage logging and independent sunspot number, TSI, seasonal temperature CZ, seasonal precipitation CZ, NAO, and seasonal NAO. The second multiple linear regression used dependent percentage of spruce logging and independent sunspot number, TSI, seasonal temperature CZ, seasonal precipitation CZ, NAO, seasonal NAO.

The data used for analyses were calculated into yearly sampled (annual) data series. Specifically, for tree rings (dendrochronological data), timber harvesting, sunspot number, and total solar irradiance (TSI) the data represent the annual mean. Precipitation, (air) temperature, and NAO data were obtained from monthly data sets. Monthly mean temperatures, monthly mean NAO, and precipitation were averaged to annual and seasonal temperatures/precipitation, respectively, to create annual data.

Calculations for "Seasonal temperature", "Seasonal NAO" and "Seasonal precipitation" were performed according to the length of the vegetation season at each plot (described in Sect. 2.2). Seasonal temperature and seasonal NAO are the arithmetic mean over the months of the vegetation season. The seasonal precipitation is the sum of precipitation during the vegetation season.

The salvage and spruce timber logging databases were expanded to include the percentage of total timber harvest. The "Percentage of spruce timber logging" and "Percentage of salvage logging" data series represent the percentage of the logging out of the total timber harvest in a single year. Percentage shares of all types of timber harvest were calculated for each year from 1961 to 2020.

Analyses for the 1961–2020 period were conducted by comparing the spruce research plots to data provided by the nearest meteorological station. Different types of timber harvests were compared with average meteorological data for the entire Czech Republic. Sunspot number and TSI were also used for the 1961–2020 period. Ring-width indices in 1900–2020 were compared with different meteorological data, unlike the case for 1961–2020. This is due to the absence of meteorological data before 1961 at local climate stations. The 1900–2020 period compares only Norway spruce plots with meteorological data from the Klementinum climate station, with sunspot numbers and TSI.

Principal component analysis (PCA) was performed in the CANOCO 5 program (Microcomputer Power) to evaluate the relations between RWI, TSI, sunspot numbers, NAO, timber harvest types, temperature, and precipitation. Before the analysis, the data were standardized and centralized. The results of PCA were illustrated by unconstrained ordination diagrams of species and environmental variables projected.

The Superposed Epoch Analysis (SEA; Chree, 1913) was calculated to reduce the importance of anomalies caused by other effects than the solar cycle. The SEA is a statistical technique used to reveal either periodicity within a time sequence or to find a correlation between two time series. Repeated events are defined as key times in the reference time series. The SEA key times were defined as the solar maximum years (maximal year mean in 1968, 1979, 1989, 2000, 2014) and determined the solar minimum years (minimum mean year in 1964, 1976, 1986, 1996, 2008). Subsets are then extracted from the second time series within a specified range around each key time and superposed to form a composite. Reference years for solar minima and maxima were determined automatically from the sunspot-number series by searching for the local minima or maxima of the sunspot-number curve. The averaging allows for the reduction of the stochastic background variability and enhancement of the possible signal synchronized with the key times. For each time in the composite, the uncertainty of the average may be computed as a root-mean-squared error of the mean.

Unfortunately, in our case only a few key epochs are identified and the composite series around the key times averages only a handful of realisations. In such a case the root-mean-squared of the mean may not properly assess the true variance of the mean.

Around the key times from the overall variability of the series, the existing autocorrelation of series was taken into account, and a Monte-Carlo-like approach was applied (Laken & Čalogović, 2013). For each time series in question, we constructed additional 1000 composites of an equal length with

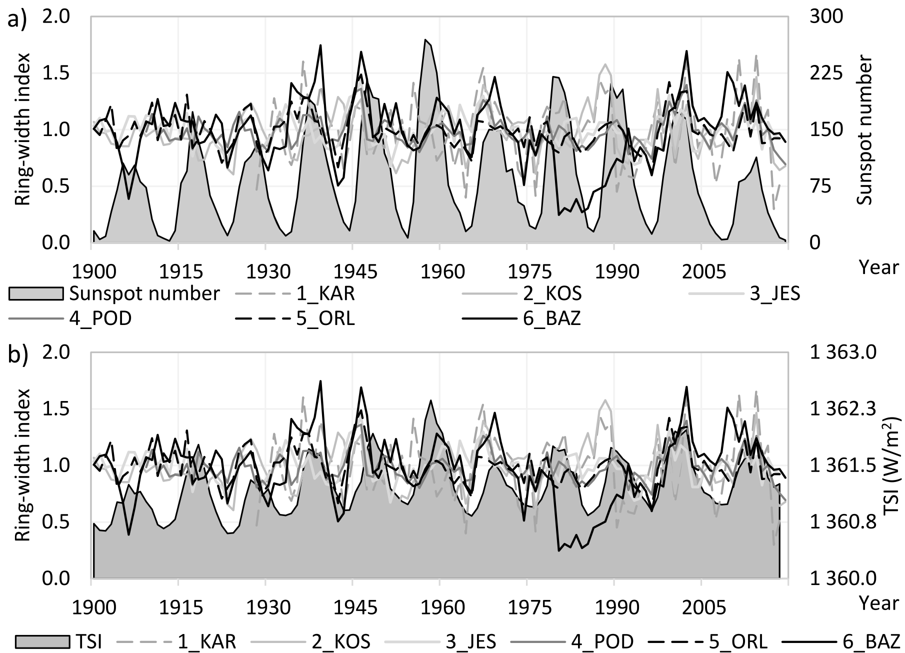

Figure 3. The time series of the ring-width index (RWI) of Norway spruce in six research plots in the Czech Republic in 1900–2019 compared with (a) The sunspot number and RWI; (b) RWI in six research plots with total solar irradiance (TSI).

randomly chosen epochs. For each time lag in the composite, we then obtained 1000 realisations of the mean, which allowed us to estimate the confidence intervals by using 5th and 95th percentile of the empirical histogram (for the chosen statistical threshold, which is $p = 0.05$). Should the mean of the reference composite at the given time lag be within the confidence interval, we cannot reject the hypothesis that the composite mean, even though it appears extreme within the composite, is due to chance. On the other hand, the mean of the composite outside the chosen confidence interval indicates a statistically significant deviation.

3 Results

3.1 Tree rings during the solar cycles

The tree-ring growth of Norway spruce undergoes numerous fluctuations. The tree-ring growth during 1900–2019 in all six research plots of this study is depicted in Figure 3, along with the sunspot number and TSI. Figure 3 reveals that RWI in all research plots roughly follows the sunspot number and TSI. The agreement appears to be somewhat better between TSI and RWI of the research plots (Fig. 3b) than between sunspot number and RWI (Fig. 3a). The RWI often shows low values during the solar minimum when the sunspot number or TSI is also lower. During the solar maximum, when the sunspot number or TSI shows higher values, the RWI also exhibits higher values. The graphs also show that there can be a decrease in RWI values before the solar maximum. This can be observed, for example, in the data from 1946 or 1990. The solar cycle is evident in the RWI of almost all the research plots, yet this phenomenon also has variations in the form of time shifts, or it can be dispersed by other factors, for instance, the air pollution calamities of the 1970s and 1980s.

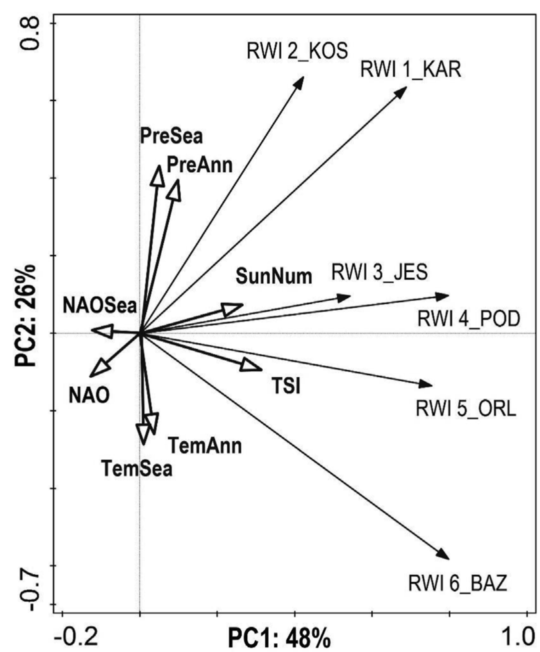

Figure 4. Unconstrained ordination diagram of species and environmental variables projected showing results of the principal component analysis of relationships between the radial width index (RWI) of individual research plots, temperature (TemAnn – annual temperature, TemSea – seasonal temperature), precipitation (PrecAnn – annual precipitation, PreSea – seasonal precipitation), total solar irradiance (TSI), North Atlantic oscillation (NAO), NAOSea – seasonal NAO and sunspot number (SunNum).

The complex relationships of the radial width index of individual research plots, temperature, precipitation, TSI, NAO, and sunspot number may be visualized by employing

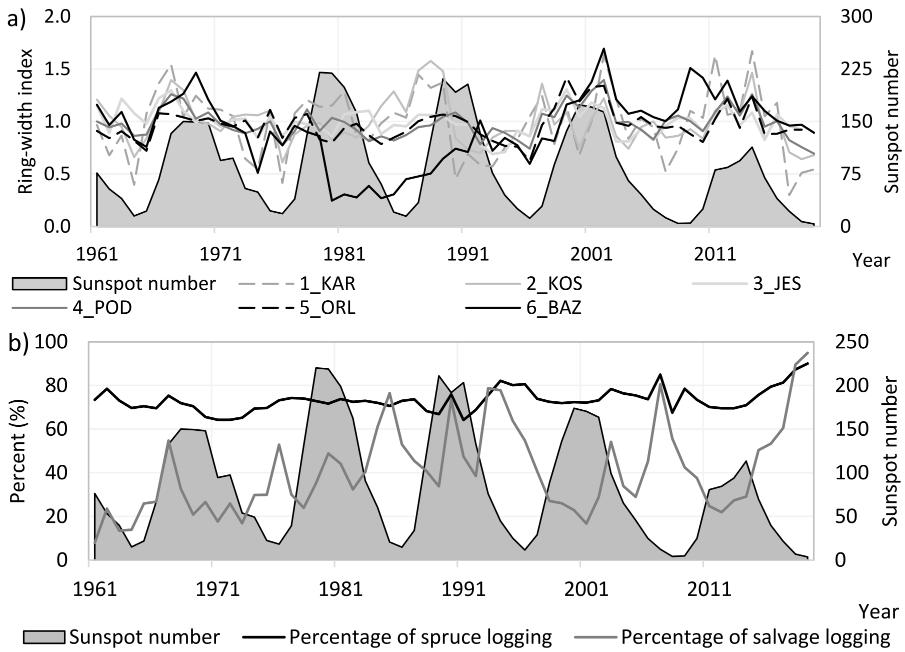

Figure 5. The change of used data from 1961 to 2019 compared to sunspot number: (a) Ring-width index (RWI) chronologies of Norway spruce on research plots in the Czech Republic; (b) Percentage of spruce logging and percentage of salvage logging.

the principal component analysis. The PCA ordinations diagram is given in Figure 4 for the period 1928–2019. The first ordination axis of PCA explains 48% of data variability, the first two axes together explain 74%, and the first four axes 95%. The total variation is 27.7, and supplementary variables account for 20.6% (adjusted explained variation 14.9%). The horizontal axis illustrates the sunspot number, seasonal NAO, and TSI, and the vertical axis depicts the temperature and precipitation data set. Precipitation and temperature in the vegetation season had greater explanatory variability than annual data. In low-altitude areas (1_KAR, 2_KOS), tree-ring growth observed a positive correlation with annual precipitation (r = 0.20 to 0.44, p = 0.01 to 0.05) and especially with precipitation in vegetation season (r = 0.21 to 0.48, p = 0.01 to 0.04). On the other hand, RWI was positively correlated with annual temperature (r = 0.20, p = 0.05) and temperature in vegetation season (r = 0.22, p = 0.04) in mountain areas (6_BAZ). However, in contrast to precipitation and temperature, the sunspot number and TSI influenced the tree-ring growth of spruce in all plots, with TSI being a highly observed indicator (r = 0.29 to 0.33, p < 0.01 on 4_POD, 5_ORL, 6_BAZ). Among the observed indicators, the NAO and seasonal NAO appear to be the least important factors influencing the RWI research plots.

3.2 Norway spruce and timber harvest

The tree-ring growth of Norway spruce since 1961 (Fig. 5a) shows that this tree species has undergone significant fluctuations. This figure describes the evolution of the percentage of spruce logging and salvage logging against the tree-ring growth in higher detail for comparison. The datasets show a common fluctuation with the solar cycle as characterized by the sunspot number (Fig. 5a). However, the common fluctuation trend of the RWI with the solar cycle is not straightforward, as shown by the

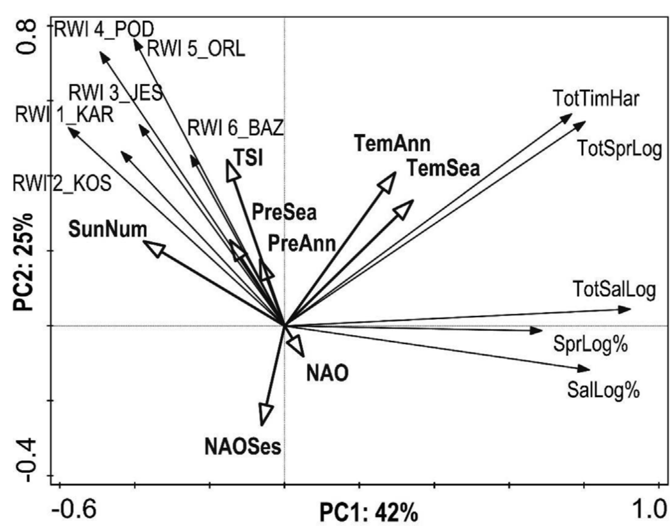

Figure 6. Unconstrained ordination diagram of species and environmental variables projected showing results of the principal component analysis of relationships between total timber harvest (TotTimHar), total spruce logging (TotSprLog), percentage of spruce logging (SprLog%), total salvage logging (TotSalLog), percentage of salvage logging (SalLog%), the radial width index (RWI) of individual research plots, temperature (TemAnn – annual temperature, TemSea – seasonal temperature), precipitation (PrecAnn – annual precipitation, PreSea – seasonal precipitation), total solar irradiance (TSI), North Atlantic oscillation (NAO) and sunspot number (SunNum).

6_BAZ research plot, which was negatively affected by air pollution in 1980–1990 (inordinately high concentrations of SO_2 from nearby power plants). Another asymmetry between

Table 4. Multiple linear regression analysis in 1961–2019 between dependent percentage of salvage logging or percentage of spruce logging and independent studied factors sunspot number, TSI, season temperature CZ, season precipitation CZ, NAO, seasonal NAO; significant results at $p < 0.05$ are in bold; seasonal temperature, seasonal precipitation, and seasonal NAO are detailed in the methodology section with the vegetation season.

	Percentage of salvage logging							
	b^*	Std.Err. of b^*	b	Std.Err. of b	t	p-value	Summary Statistics	
Intercept			49044.13	22708.36	2.16	0.04	Multiple R	0.47
Sunspot number	0.28	0.27	0.08	0.08	1.04	0.30	Multiple R^2	0.22
TSI	−0.59	0.28	−36.09	16.71	−2.16	0.04	Adjusted R^2	0.12
Seasonal temperature CZ	0.38	0.17	7.61	3.48	2.19	0.03	F	2.35
Seasonal precipitation CZ	−0.05	0.16	−0.01	0.05	−0.29	0.77	p-value	0.04
NAO	0.23	0.19	7.55	5.98	1.26	0.21	Std.Err. of estimate	17.77
Seasonal NAO	−0.21	0.18	−5.55	4.56	−1.22	0.23		
	Percentage of spruce logging							
	b^*	Std.Err. of b^*	b	Std.Err. of b	t	p-value	Summary statistics	
Intercept			−4992.04	5684.31	−0.88	0.38	Multiple R	0.50
Sunspot number	−0.54	0.27	−0.04	0.02	−2.04	0.04	Multiple R^2	0.25
TSI	0.24	0.27	3.71	4.18	0.89	0.38	Adjusted R^2	0.17
Seasonal temperature CZ	0.25	0.17	1.29	0.87	1.48	0.84	F	2.89
Seasonal precipitation CZ	0.11	0.16	0.01	0.01	0.72	0.51	p-value	0.02
NAO	0.04	0.18	0.30	1.50	0.20	0.15	Std.Err. of estimate	4.45
Seasonal NAO	0.11	0.17	0.76	1.14	0.67	0.48		

Notes*:* b^* – standardized and b – non-standardized regression coefficients (relative contribution of each independent variable); Std.Err. – standard error; t – the t-value and resulting p-value are used to test the hypothesis that the intercept is equal to 0; F – the F-value and resulting p-value is used as an overall F-test of the relationship between the dependent variable and the set in independent variables.

tree-ring growth and the solar cycle is evident in 1989 for the research plots of 1_KAR and 2_KOS. All plots show the RWI concurrent with the solar cycle from 1961 to 2019. However, there are exceptions that disperse the concurrence of the RWI with the solar cycle at individual plots.

The percentage of spruce timber logging also indicated common fluctuation trend with the solar cycle, which is clearly visible in Figure 5b. This figure shows that in recent years, there has been a higher amount of total logging in spruce stands. The percentage of spruce timber logging does not precisely follow the solar cycles, but there is a hint of a common fluctuation trend. The percentage of salvage logging in Figure 5b has been distinctly following solar cycles since 1994, with previous years showing more frequent peaks of salvage logging.

The complex interactions between the timber harvest, radial width index of individual research plots, temperature, precipitation, TSI, NAO, and sunspot number are shown in Figure 6 for the period 1961–2019. The first ordination axis of PCA explains 42% of data variability, the first two axes together explain 67%, and the first four axes are 85%. Total variation is 696.0, supplementary variables account for 34.3% (adjusted explained variation 23.6%). The sunspot number was negatively correlated ($p < 0.05$) with all timber harvest types ($r = -0.35$ to -0.44). Annual and seasonal temperatures were positively correlated ($r = 0.46$ to 0.51; $p > 0.05$) with all timber harvest types except the percentage of salvage logging. Precipitation has less effect on harvest indicators ($r = -0.25$ to 0.03). Radial width indices were negatively correlated ($r = -0.28$ to -0.48; $p > 0.05$) with total salvage logging, percentage of spruce logging, and percentage of salvage logging. Generally, temperature, sunspot number, and TSI were more explanatory variables in the context of radial growth and timber harvest types compared to low-effect NAO and precipitation. Even though seasonal NAO exhibited a more noticeable negative relationship with logging compared to RWI, it did not indicate high r values for our assessed timber harvests ($r = -0.07$ to -0.12).

The application of multiple linear regression (MLR) analysis, detailed in Table 4, complements the findings from Principal Component Analysis (PCA). For the percentage of salvage logging, the MLR model yields an overall multiple R of 0.47, with a statistically significant intercept ($p = 0.04$). Among the variables considered, TSI exhibits the most substantial influence, indicated by a coefficient (b^*) of −0.59. Additionally, seasonal temperature has a significant impact, with a b^* of 0.38 at $p = 0.03$. In summary, in predicting the percentage of salvage logging, TSI plays a prominent role in the MLR analysis, followed by seasonal temperature.

For the percentage of spruce logging, the MLR model shows a slightly higher multiple R of 0.50 compared to the salvage logging case. However, the intercept is not statistically significant. Among the independent variables, the sunspot number holds the highest coefficient (b^*) of −0.54, with the sole significant p-value of 0.04.

3.3 Feedback of solar cycles to tree rings and timber harvest

The application of the SEA (superposed epoch analysis) method to datasets of RWI and percentage of salvage logging and percentage of spruce logging (Fig. 7) reveals patterns during the solar maximum and minimum in the period 1961–2019. The SEA analysis describes the average course of the examined data during selected epochs in solar maximum or minimum.

The RWI behaves differently during solar maxima and minima. During solar maxima at Lag 0, there are varying increases in RWI for each research plot (mean RWI = 1.0–1.3). It can be

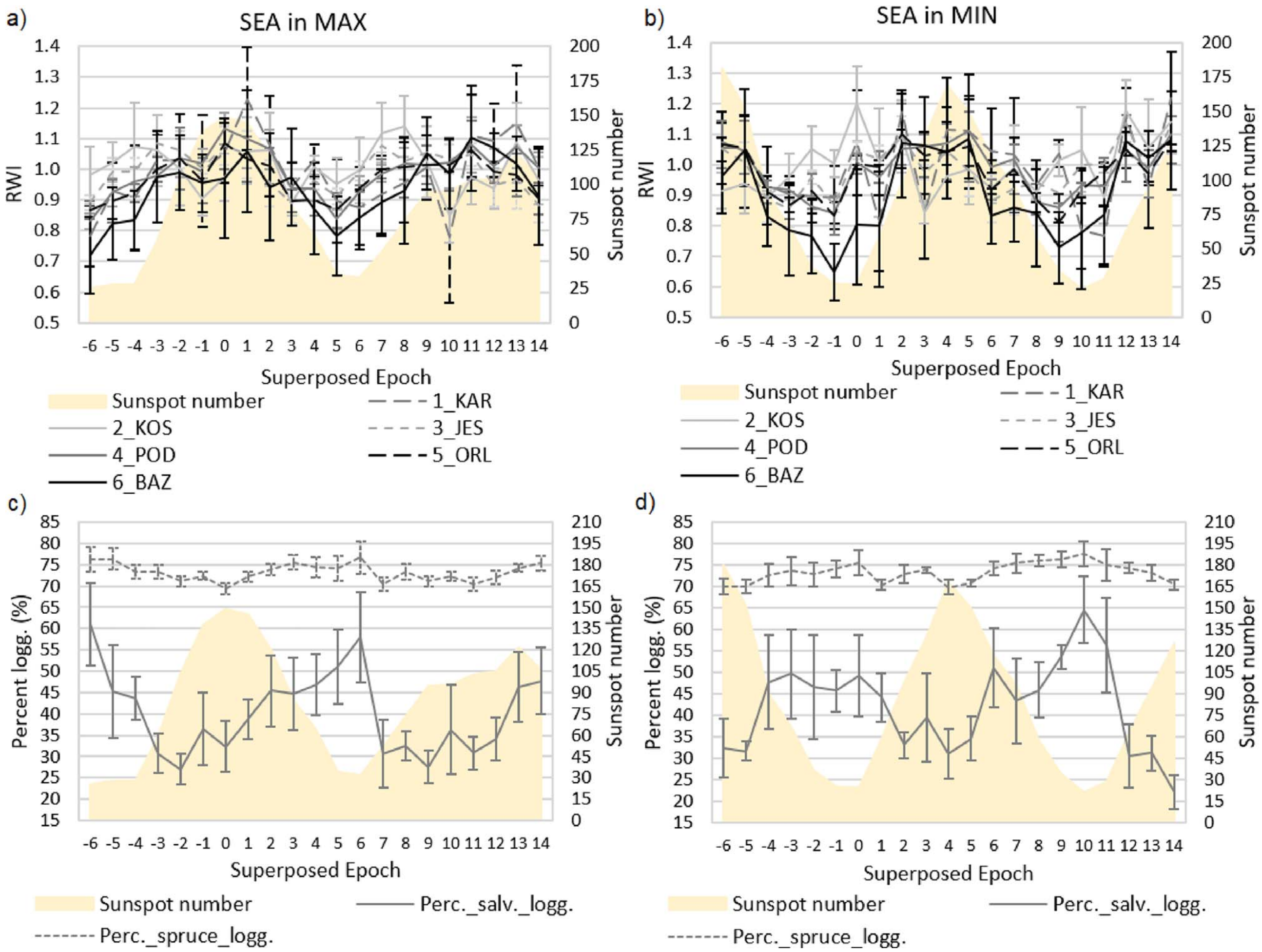

Figure 7. Plots of epoch-superposed subsets in 1961–2019 from solar maximum (max) and solar minimum (min) in relative −6 years before and 14 years after the key epoch; RWI research plots in max a) and in min b); percentage of spruce logging and percentage of salvage logging (logg.) in max c) and in min d); the error bars show the one-standard-deviation half-widths.

observed that during solar maxima, there are variable increases in spruce RWI, but the overall growth reaches in each plot peaks mostly from Lag −2 to Lag 2 (mean RWI = 0.95–1.08) with the largest RWI observed in Lag 1 (mean RWI = 1.05–1.24). During solar minima, all research plots experience the lowest RWI at mostly Lag −1 (mean RWI = 0.66–1.02). A synchronized gradual decline in RWI from Lag −6 (mean RWI = 0.92–1.08) across all research plots is observed as well. From Lag −1 (mean RWI = 0.66–1.02), there is an increase in RWI for all research areas, continuing until Lag 2 (mean RWI = 1.06–1.18).

The percentage of spruce logging during solar maxima SEA has its lowest percentage at Lag 0, which is in the range of 68–71%, and the highest logging occurs at Lag 6, reaching at range 73–81%. However, during solar minima, the percentage of spruce logging exhibits its highest values directly at Lag 0, with range of 72–82%. As we move away from Lag 0 in SEA min, the percentage of spruce logging decreases, with logging values irregularly decreasing until Lag 3 to range 68–70%. On the other hand, a gradual and regular decline in the percentage of spruce logging in SEA minimum is observed as we move into the negative Lag −5 with a range 69–71%.

The percentage of salvage logging exhibits greater variations in logging during the cycle than the percentage of spruce logging. During solar maxima, the percentage of salvage logging shows its lowest values mostly at Lag −2 with a range of 24–30%. Overall, the percentage of salvage logging during solar minima records its highest value at Lag 0, reaching the range of 39–59%. From Lag 0 in SEA minimum, salvage logging irregularly decreases on both the positive and negative sides of Lag, similar to the percentage of spruce logging. In the SEA minimum for logging from Lag 10% of spruce logging is in the high range of 75–81% and the percentage of salvage logging is in the high 18 range of 57–73%.

3.4 Spectral analysis of timber harvests and tree rings in 1961–2019

The single spectral analyses in Figure 8 show an example of RWI plot 4_POD and 6_BAZ cyclical relationships in Norway spruce indexed tree rings for the period 1900–2019. The rest of the research RWI plots are very similar to the examples. The exceptions are the research plots 4_POD (age 112 years) and 1_KAR (age 92 years), which have a shorter age period. The

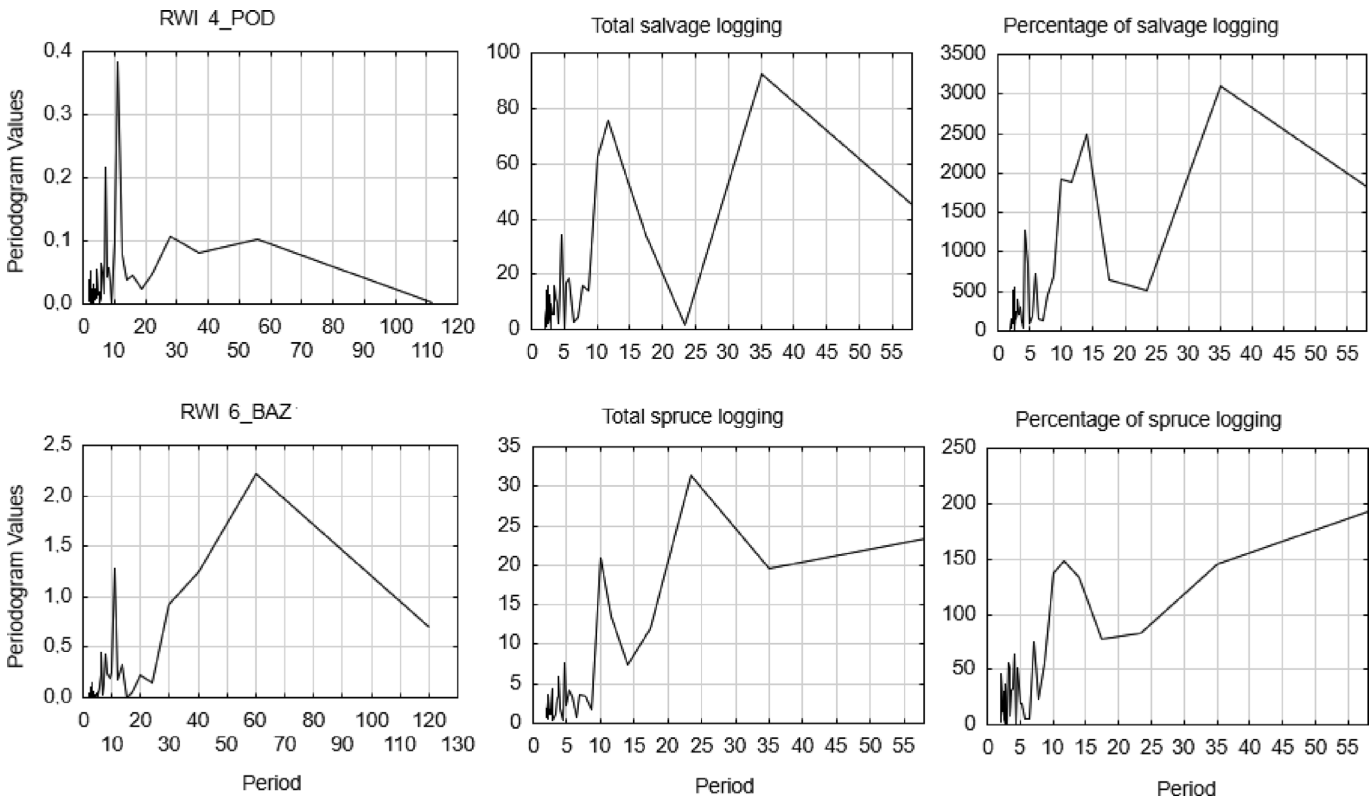

Figure 8. Single spectral analysis of used datasets, ring-width indixes (RWI) in 1900–2019 for RWI, and types of timber logging in 1961–2019.

periodogram values show the variance of the data at the respective period. Ring-width indices (RWI) from each Norway-spruce research plot show 9-year to 14-year cycles in their tree-ring growth. Furthermore, four of the six research plots show 35-year cycles, which generally have lower periodogram values than the 9-year to 14-year cycles. The exception is the 6_BAZ research plot, which shows higher periodogram values for 60-year cycles. However, even the 6_BAZ research plot has an 11-year cycle in its tree-ring growth.

Timber harvest types in Figure 8 have also experienced 10-year to 14-year cycles, similar to the RWI. However, timber harvest types from 1961 to the present day have a shorter period. Regarding cyclicity, the total, coniferous, and spruce timber harvests have the most similarities, showing the same 10-year and 25-year cycles. Salvage logging follows 11-year and 35-year cycles, evidenced by spectral analysis. The percentage of salvage logging and spruce timber logging indicate 10-year to 14-year cycles and 35-year cycles, respectively. Observed RWI and harvest data show a peak at around the 11-year cycle in spectral analysis.

4 Discussion

4.1 Anthropogenic and meteorological influences in logging

Norway spruce is sensitive to weather extremes (Tumajer et al., 2017; Netherer et al., 2019). The Czech Republic also suffered from excessive sulphur dioxide deposition in the 1970s and 1980s, created by the flue gas from coal-fired power plants (Mikulenka et al., 2020; Šimůnek et al., 2021a). This negatively affected tree growth, primarily in the highest parts of the mountainous areas (Matějka et al., 2010; Vacek et al., 2015a; Šimůnek et al., 2019). The 6_BAZ research plot (Fig. 3a) responded with a sharp drop in RWI to the period of the air pollution calamity (1980–1990). This RWI drop is most evident at the highest altitude research plot of 6_BAZ, which is illustrated in Figure 5a. This reduction in increment, induced by air pollution, led to forest dieback in the area and an increase in deadwood (Vacek et al., 2015b). Air pollution also had an impact on the salvage, total, spruce, and coniferous timber harvests in other mountainous areas, evidenced in Figure 5, as an average of 6.2 million m^3 of timber was harvested in salvage loggings. As a result of the air pollution disaster, about 47,300 m^3 of timber was logged in the mountainous areas of the Czech Republic, i.e., a total of 2% of the Czech forest area, primarily in the Krušné hory, Lužické hory, Jizerské hory, Krkonoše, and Orlické hory Mountains (Vacek et al., 2003).

Drought, coupled with rising temperatures, particularly in recent years, has been identified as a contributing factor to increased salvage logging in spruce stands (Netherer et al., 2019). The multiple linear regression analysis in Table 4 underscores seasonal temperature as a significant factor (p = 0.03) influencing salvage logging. In contrast, there is no apparent link between seasonal precipitation and salvage logging as indicated by the multiple linear regression analysis. One possible explanation for this could be the upsurge in salvage logging following windstorms and bark beetle overpopulation in deciduous forests.

The process of salvage logging, in turn, modifies the microclimate of the plot (Peterson & Leach, 2008). Elevated temperatures contribute to more frequent bark beetle swarming, leading to additional generations within a single season (Marini et al., 2013). Consequently, this escalation in salvage logging is reflected in the overall logging of spruce timber (Marini et al., 2017).

Precipitation is linked with tree-ring growth, especially at lower altitudes in the 1_KAR and 2_KOS research plots, that faced more frequent drought periods in this region and are (Fig. 4) accompanied by low RWI (Fig. 5) in recent years. At lower elevations, Norway spruce is more negatively affected by irregular precipitation during the vegetation season than at higher altitudes (Rybníček et al., 2012), which significantly increases salvage logging in the Czech Republic (MAF, 2021). During drought periods, *Ips typographus* reproduce excessively and infest healthy trees too (Schroeder & Lindelöw, 2002; Turčáni & Hlásny, 2007). It is a necessary time to remove infested epicenters from the forest before the bark beetle increases its numbers and attack other mostly nearby trees (Økland & Berryman, 2004).

The challenges surrounding timber extraction in the Czech Republic are exacerbated by the aging of forest stands. Thanks to the Forestry Act in the 1990s, the rotation period of forests in the Czech Republic was extended. This resulted in forests aging from 102 years in 1960 to 114 years in 2018. It is precisely this increase in the age of forest stands that made them more susceptible to climate fluctuations (Šimůnek et al., 2020b). As forest stands age is higher, the occurrence of windthrow and bark beetle infestations becomes more frequent. Research has shown that the risk of disturbances in these stands increases with the higher age of forest stands (Nascimbene et al., 2013). This is further supported by the observed higher salvage logging activities in the late 20th and early 21st century (Fig. 2a). Therefore, salvage logging is continuing higher also in percentage (Fig. 5b).

Furthermore, the complexity of 20th-century calamity dynamics is compounded by the change in ownership of smaller forest properties, which were restituted during the 1990s (Fig. 1c). Many of these smaller properties are owned by individuals who cannot effectively harvest and manage broken and infested wood. As a result, the populations of bark beetle pests proliferate, gaining strength and causing further damage (Zahradník & Zahradníková, 2019; MAF, 2021). The inability to process harvested timber from salvage logging time is evident in our data regarding the percentage of salvage logging. Before 1995, there were higher frequencies of wood processing, but, for example, since 2000, the calamities have been longer and much more intense. The inability to process wood is also related to the reduced number of employees in forestry, which only complicates the processing of random timber harvesting (Seidl et al., 2016).

4.2 Spruce tree rings and timber harvest comparison to the solar cycle

The sunspot cycles represented by the sunspot number and TSI observed link with all logging types from 1961 to 2019. Multiple linear regression analysis of our results (Table 4) showed a notable link between the percentage of spruce logging with a sunspot number. The PCA in Figure 6 revealed a strong positive link between RWI and the studied types of timber harvests, as well as TSI and sunspot number. A recent study described this phenomenon in the Czech Republic, where salvage logging observed correlation ($p < 0.05$) with the sunspot area (Šimůnek et al., 2020b). Solar cycles have also been confirmed in other European locations on the annual rings of other important forest tree species, such as Scots pine (*Pinus sylvestris* L.) – (Shumilov et al., 2011; Matveev et al., 2017; Kasatkina et al., 2019) or European beech (*Fagus sylvatica* L.) (Šimůnek et al., 2020a; Komitov, 2021). We hypothesize that increased solar activity, characterized by a higher sunspot number and larger total solar irradiance (TSI), enhances tree growth (as reflected in increased RWI), which may subsequently influence bark beetle infestations and trigger changes in logging practices.

While the impact of TSI is significant for tree rings and timber harvests, particularly influencing RWI in research plots (see Fig. 4), it is intricately connected with the sunspot number. The connection between sunspot number and TSI is complex when compared to various solar parameters indirectly linked to tree rings. TSI itself undergoes a 0.1% variability (approximately 0.08 ± 0.2 K) over an 11-year cycle, reaching its peak during solar maxima (Kopp, 2021). As the sunspot number increases, so does the TSI, resulting in a higher level of UV radiation. However, the effects of the solar cycle are multifaceted, involving the broader solar spectrum. Notably, the entire light spectrum varies with the solar activity cycle (Tsiropoula, 2003; Yeo et al., 2017). To comprehend this intricate interplay between solar dynamics and our climate indicators, it is crucial to explore the combined influence of TSI, spectral variations, and the many other solar components.

Our results of multiple linear regression (Table 4) suggest an important role ($b^* = -0.59$ at $p < 0.04$) of TSI with the percentage of salvage. Thus, TSI has slightly a greater effect on RWI and types of loggings than sunspot number according to the Figures 4 and 6 (PCA). The TSI with RWI can be linked to the influence of UV radiation of the Sun, which also changes throughout the solar cycle (Floyd et al., 2002, 2003). The UV (more precisely UV-B) radiation can influence tree ring growth by inducing oxidative stress in trees, which can lead to narrower tree rings (Madronich, 1993). Additionally, increased UV-B radiation can stimulate the production of secondary metabolites like lignin and flavonoids in response to stress, potentially affecting ring patterns (Ballaré et al., 2001).

Our PCA results for RWI also indicate the same variability with respect to the sunspot number and TSI. The effect of TSI on climate has been indirectly associated with the South Asian summer monsoon cycle, which is imprinted in tree rings (Shi et al., 2014). Our results also revealed that TSI and temperatures are associated with RWI, where according to the PCA (Fig. 4), the influence of temperature on RWI increases with increasing altitude. The impacts of irradiance and radiation variations on spruce tree rings are significantly higher at mountain altitudes compared to spruce trees in lowlands (Černý et al., 2020). This is also supported by results from regression analysis where even the percentage of salvage logging observed an important link with TSI and temperature while the main portion of the salvage loggings are from middle and high altitudes. There is also the assumption that temperature is less influenced by the solar cycle influences than precipitation in North-Eastern Europe

(Chapanov & Gorshkov, 2019). Therefore, there is an inclination to the fact that the temperature initiates higher timber harvests, which is a long-term trend longer than the solar cycle. We suggest that the presence or absence of precipitation – whether in the form of drought or wet periods – has an immediate impact on salvage logging, resulting in either a decrease or increase in the volume of harvested timber. Consequently, we hypothesize that the patterns of these dry and wet periods affecting the health status of the trees are likely linked to some mechanism associated with the solar cycle.

According to the SEA shown in Figure 7, the spruce research plot's RWI has mostly the higher variable growth around solar maximum, indicating that the tree-ring series growth was associated with the solar cycle through indirect climate effects. However, during solar minima, the lowest RWI at Lag −1 is observed mostly across all research plots, and a synchronized gradual decline in RWI is mostly observed from Lag −5 onwards across all research areas. This may indicate that the average RWI is influenced by a climatic feedback mechanism associated with the solar cycle. Similar results between observed lags of sunspot number and RWI were found in European beech in the Krkonoše Mountains and Broumov region in the northeast Czech Republic (Šimůnek et al., 2021b). These observed lags are likely to be associated with the NAO, which influences precipitation and temperatures in Europe (Wibig & Piotrowski, 2018; Kotsias et al., 2020). Our results show that, among the considered factors, NAO contributes to RWI to the least extent according to PCA (Fig. 4). However, in the PCA (Fig. 6) for timber harvesting, it is evident that seasonal NAO may play a role in climate-related factors influencing timber harvesting while the multiple linear regression analysis did not confirm any strong evidence.

Before the peak of percentage spruce harvesting and percentage salvage logging, all RWI plots, according to SEA analysis, exhibited their lowest values mostly at Lag −1, which is one year prior to the solar minimum. However, during the solar maximum, significant long-term calamities were not recorded, and even in the recent 30 years, the interval between calamities has extended further according to the 11-year cycle. This difference between RWI and timber harvests is due to the chronic weakening of spruce stands, which is indicated by higher salvage logging due to increased vulnerability for forest stands (Kolář et al., 2017) This low tree-ring growth can be an early warning indicator of extensive spruce stand disintegration along with other indicators such as the abundance of *Ips typographus* populations (Marini et al., 2017).

The solar cycle is firstly observed in the tree-ring growth of spruce, and then, with a 1-year delay, will manifest itself in the percentage of salvage logging while RWI in the solar maximum is not significantly stressed. According to the multiple linear regression analysis, a significant relationship was even found between sunspot numbers and the percentage of spruce logging, indicating that logging activities can be linked to solar cycle related changes in temperature and precipitation in the Czech Republic. Some studies describe bark beetle infestations in relation to solar radiation and its effect on the habitat, especially during the peak and decline phases of the beetle outbreak (Mezei et al., 2019). This link between TSI and calamities may relate to a higher infestation of the forests, which slightly prolongs the vegetation season effect on higher tree-ring growth. A mostly one-year preceding Lag indicated low tree rings to sunspot minimum and with a maximal salvage and spruce logging is something new. This Lag effect may be due to sudden stratospheric warming events (SSWs), altering stratospheric circulation and affecting the jet stream, storm paths, rainfall, and temperatures. During solar minimum/easterly QBO years, midwinter SSW frequency slightly increases (0.67 per year at 90% confidence). However, study observations alone cannot confirm the robustness of the solar-QBO-SSW relationship (Baldwin et al., 2021). The apparent observation of a solar cycle in RWI and timber harvests may be a false attribution to the solar cycle due to the sparse database of a few solar cycles. Even, artificial (false) solar fluctuations correlations and coherences may be even higher than, those generated by genuine solar variability in for example we found that this was observed in QBO phases (Salby & Shea, 1991).

Solar activity can induce changes in temperature and pressure, influencing the dynamics of the atmosphere and correlating with fluctuations in the NAO. These similarities can also be identified over decadal periods, with a Lag of a few years relative to the solar cycle. Some studies emphasize that solar variability can impact atmospheric circulation, interacting with pressure systems and manifesting in decadal NAO signals (Scaife et al., 2013; Gray et al., 2017; Ye et al., 2023). Overall, it can be concluded that there is a connection between solar variability and decadal changes in the NAO over Europe, and from our data used in Figure 2, the coincidence of fluctuations between the NAO and the sunspot number can be visually observed, mainly since the 1980s until the present.

The NAO phases are probably an important reason why we can observe such cycles on tree rings and types of timber harvesting (Fig. 6). The NAO varies between positive and negative phases, which can be identified as potential drivers affecting forest growth and timber harvesting in Central Europe. The NAO, with its distinct phases, can introduce varying weather patterns that influence temperature and precipitation. These variations can be observed in tree-ring data, influencing the radial growth of trees. The NAO phase is linked to the formation of distinct climate patterns and atmospheric pressure systems, which can influence tree-ring series in the region. The complex interaction between NAO phases, the solar cycle, and their effects on tree-ring series and timber harvesting has been the subject of extensive research (Jones et al., 1997; Piovesan & Schirone, 2000; Trouet et al., 2009; Leonelli et al., 2017). The connection between the NAO, the solar cycle, tree-ring series, and timber harvesting in Central Europe is a multifaceted relationship, and understanding these interactions contributes to a more comprehensive insight into the region's forest ecosystems.

4.3 Cyclical presence of the solar cycle on spruce from rings to timber harvest

The results of the spectral analyses (Fig. 8) recorded high similarity to the 11-year cycle for almost all the time series from RWI to different types of timber harvest. There is an assumption that solar-induced changes in the atmosphere might be the reason of observed results, but the solar cycle does not always last the same length of time (Chiodo et al., 2012, 2019; Scafetta, 2012; Hathaway, 2015). The solar cycle is present in the RWI from all research plots, as shown by the results of PCA from 1900 to 2019 (Fig. 4). All harvest types also show an 11-year cycle in the data, which is most evident in the salvage logging (Fig. 8). And it is the salvage logging that take place concurrently to the solar cycle (Šimůnek et al., 2020b), which is confirmed by the results with percentage of salvage logging. Norway spruce harvest indicates common fluctuation trend to the solar cycle, but the concurrence is not as clearly visible as in the case of salvage logging. In our results, the solar cycle manifests in various forms, ranging from tree rings to timber harvesting. However, it is essential to note that these signals may not be solely attributed to a pure solar source.

The presence of the solar cycle in our data is influenced by climatic factors that are likely remotely linked to the NAO. Although this phenomenon was not statistically supported by regression analysis, the tree-ring series, as analyzed through PCA, shows a relationship with the seasonal NAO. The alternation of NAO phases in Central Europe is significantly impacted by the solar cycle. During the positive phase of the NAO, there is a higher occurrence of cloudy days, reducing solar radiation (Foukal et al., 2006). Conversely, during the negative phase of the NAO, there are typically more sunny days, promoting increased solar radiation and a positive impact on the solar cycle (Lockwood et al., 2014). Therefore, we argue that the influence of TSI can be observed in our datasets.

Additionally, the results related to the percentage of spruce timber logging are significant to sunspot number (Table 4). Spruce timber logging also follows a longer, 58-year cycle, partially visible in Figure 8, which is consistent with the natural growth and commercial rotation of Norway spruce, which undergoes these cyclic disturbances (Mikol et al., 2020; Vacek et al., 2021). Before the 1990s, the cyclical rotation of spruce forest harvesting in the Czech Republic was around 80 years, but then it was increased to almost 115 years of the age of the forest stands, which is partly reflected in the trend of total and spruce timber harvesting (Remeš et al., 2020). Medium-term 25-year cycles are observed for total, spruce timber, and coniferous timber logging (Fig. 8). In terms of numerical similarity, this cycle could be related to the 22-year Hale cycle, which recurs through meteorological indicators such as precipitation (Laurenz et al., 2019) and temperature (Lüdecke et al., 2020). Similar cyclical results to our study were also recorded in the tree-ring growth of Scots pine in the western Russian steppe, where 10–12-year, 22-year, and 32–36-year cycles were recorded. This 35-year cycle can be defined according to the Brückner-Egeson-Lockyer cycle, which is associated with climatic fluctuations that are documented in climatic indicators (Halberg et al., 2010). There were even 70–90-year fluctuations in the moisture regime (Matveev et al., 2017).

In the conditions of the Czech Republic, the solar cycle manifests itself first on spruce that has been weakened by drought and cyclical worsening of growing conditions, which is well shown in Figure 5, where the RWI of spruce at the research plots reacts cyclically with the solar cycle. During periods of poor growth conditions, spruce trees are physiologically affected by higher temperatures and lack of precipitation (Rybníček et al., 2010; Tumajer et al., 2017). It is related to the solar cycle through variability in the irradiance at the Earth's surface (Dasi-Espuig et al., 2016; Kopp et al., 2016), lack of precipitation during the growing season (Laurenz et al., 2019), and fluctuations in temperatures (Lüdecke et al., 2020). All of this is related to air circulation, manifesting in windy calamities. At the same time, there is a gradual overpopulation of bark beetles which increases salvage logging (Šimůnek et al., 2020b).

Our results show a repeatable pattern similar in the RWI and timber harvests to the 11-year solar cycle on the seasonal weather regime that is probably linked with drought period in which trees are sensitive. River Ammer (southern Germany) flood frequency variability and summer extreme events were observed in seasonal data in central Europe, which can be explained by a solar modulation of eastern European-western Russia summer blocking and associated upstream upper-level wave-breaking activity (Rimbu et al., 2021).

4.4 Opportunities and challenges in the declining of spruce forests: understanding limitations and potential outcomes

Wind, bark beetle, and air pollution disturbances primarily increase salvage, total, spruce timber, and coniferous timber logging in the Czech Republic (Hlásny & Turčáni, 2013; Mitchell, 2013; Vacek et al., 2013; Hlásny et al., 2014). The substantial increase in percentage (Fig. 7) of Norway spruce logging grows from a mean of 69% (range 68–71%) to a mean of 77% (range 73–81%.) and the percentage of salvage logging is from mean 35% (range 22–42%) to 60% (range 47–69%) from the solar maximum to solar minimum. In Figure 3, our data describe that spruce is cyclically stressed, as apparent in the concurrent low RWI. Increased spruce logging follows, and simultaneously, the salvage logging increases too (e.g., around 2007 or 2019). The rise in spruce timber logging exerts significant pressure on the forestry sector, which is forced to sell high volumes of timber within a short period of time. This destabilizes market prices of timber (Jandl, 2020; Hlásny et al., 2021b).

Coniferous forests are consequently susceptible to a range of secondary diseases and pests and are particularly vulnerable to warmer and drier climates (Seidl et al., 2008). The overall situation is exacerbated by the lower quality of timber, damaged by windthrows and bark beetles (Kärhä et al., 2018; Netherer et al., 2019). However, the decline of spruce forests provides more space and support for European beech, which is more adaptable to climatic fluctuations than Norway spruce (Kolář et al., 2017; Vacek et al., 2019, 2021). Considering that salvage logging and timber harvesting occur in cycles similar to the eleven-year solar cycle, we suggest these cycles might affect the wood industry. Given the impact of these cycles on forestry, we could use this knowledge for long-term planning in the timber and forestry sectors.

However, the tree-ring growth does not always coincide with the solar cycle. This is apparent from 1900 to 1919 when the trees were not stressed due to a lack of precipitation (Fig. 2c). During this period, there was a more stable distribution of precipitation and temperature across the Czech Republic, particularly during the vegetation season. During this time, the RWI does not exhibit a clear solar cycle pattern in nearly all plots. The RWI has notably decreased since 1980 at the 6_BAZ research plot during the human-induced air pollution period.

Internal decadal variability of the climate system, incorporating TSI, sunspot number, and the NAO, can exert significant influence. For example, TSI is associated with sunspots, affecting temperature patterns (Usoskin et al., 2016). Simultaneously, NAO has the potential to influence regional climate by impacting precipitation and temperature distributions, particularly in Northern Europe. Higher temperatures and altered precipitation regimes can affect tree growth, showing a positive response in certain circumstances (Carrer & Urbinati, 2004). Nevertheless, our data display a lag in RWI response, like a reduction a year before the maximum timber harvests, possibly attributed to the influence of NAO (Helama et al., 2009). The NAO, by affecting moisture availability, can either dry or moisten the climate in Central Europe, creating conditions unsuitable for tree growth (Cook et al., 2010).

5 Conclusion

Norway spruce harvest is one of the primary forestry activities in the Czech Republic. It becomes apparent that climatic fluctuations greatly affect spruce timber harvesting, as do cyclical calamities. The ring-width indices of Norway spruce from six research plots indicate a relationship between timber harvesting and its RWI. The types of loggings are greatly influenced by temperatures, seasonal NAO, and TSI. Regarding the percentage of spruce logging, the sunspot number was the highest indicator on the multiple linear regression analysis. Percentage of salvage logging is significantly linked to TSI and seasonal temperature. The average RWI series reveals predominantly low tree ring growth with a lag time of one year prior to the occurrence of the maximal timber harvests. Timber harvests are higher during Lag 0 with the solar minimum when spruce and salvage logging typically peaks and then decreases to solar maximum. Spruce logging and tree-ring series show a close yet not fully and precisely described relationship with the 11-year solar cycle. The results of this study can help to understand the cyclical relationships between spruce tree rings and the management of this tree species. A comprehensive view of cyclical fluctuations in forestry can assist forest management to better prevent unexpected calamities in the future and thus reduce the impacts of climate change. The findings of this study can be applied to improve action against major forest calamities in Central Europe. Nevertheless, a more in-depth investigation of this topic is essential for its future application.

Acknowledgements

We would like to thank Richard Lee Manore, a native speaker, and Jitka Šišáková, an expert in the field, for checking English. We are also grateful to the Czech Hydrometeorological Institute of the Czech Republic (CHMI) for providing the climate data of precipitation and temperature https://www.chmi.cz/; to the Royal Observatory of Belgium (WDC-SILSO) for providing the annual (yearly mean) sunspot number sunspot number data at https://www.sidc.be/silso/, to Climatic Research Unit, University of East Anglia (CRU-UEA) for providing the monthly NAO value data at https://crudata.uea.ac.uk/cru/data/nao/ and to Greg Kopp for his publicly available TSI data at https://spot.colorado.edu/~koppg/TSI/. We also thank the Forest Management Institute (ÚHÚL) in Brandýs nad Labem at https://www.uhul.cz/portfolio/poskytovani-dat/ (Czech Republic) and the Czech Statistical Office (CZSO) in Prague at https://www.czso.cz/, Czech Republic, for providing data on timber harvests in the Czech Republic. The editor thanks Tobias Spiegl and an anonymous reviewer for their assistance in evaluating this paper.

Funding

This study was supported by the Czech University of Life Sciences Prague, Faculty of Forestry and Wood Sciences (Excellent Output 2021–2022), and the Ministry of Agriculture of the Czech Republic, Project No. QK21010198, Adaptation of forestry for sustainable use of natural resources. M.Š. was supported by the institutional support of the Czech Academy of Sciences under project RVO:67985815.

Conflicts of interest

The authors declare that they have no known competing financial interests or personal relationships that could have appeared to influence the work reported in this paper.

Data availability statement

Climate data on precipitation and temperature used in this study are available from the Czech Hydrometeorological Institute (CHMI) at https://www.chmi.cz/. North Atlantic Oscillation (NAO) index data are from Climatic Research Unit, University of East Anglia at https://crudata.uea.ac.uk/cru/data/nao/. Sunspot number data can be accessed through the Royal Observatory of Belgium (WDC-SILSO) at https://www.sidc.be/silso/. Total Solar Irradiance (TSI) data provided by Greg Kopp are available at https://spot.colorado.edu/~koppg/TSI/. Data on timber harvests in the Czech Republic were provided by the Forest Management Institute (ÚHÚL) in Brandýs nad Labem at https://www.uhul.cz/portfolio/poskytovani-dat/ and by the Czech Statistical Office (CZSO) in Prague at https://www.czso.cz/.

Author contribution statement

V.Š. initiated and designed the study and its methodology, collected samples, analyzed the data, and wrote and edited the first draft of the manuscript. Z.V. analyzed the data, prepared the first draft of the manuscript, and participated in the review process. S.V. contributed to the design of the study and the first draft of the manuscript. V.H. made field measurements and sampling and contributed to data analysis. G.D. made field measurements, collected samples, measured and analyzed the data, and participated in the preparation and review of the manuscript. M.Š. performed SEA analysis, discussed the Sun-related issues, and participated in the preparation and review of the manuscript. All contributing authors have read and agreed to the version of the published manuscript.

References

Akhmetzyanov L, Sánchez-Salguero R, García-González I, Domínguez-Delmás M, Sass-Klaassen U. 2023. Blue is the fashion in Mediterranean pines: New drought signals from tree-ring density in southern Europe. *Sci Total Environ* **856**: 1–15. https://doi.org/10.1016/j.scitotenv.2022.159291.

Alvarez S, Ortiz C, Díaz-Pinés E, Rubio A. 2016. Influence of tree species composition, thinning intensity and climate change on carbon sequestration in Mediterranean mountain forests: a case study using the CO2Fix model. *Mitig Adapt Strateg Glob Chang* **21**: 1045–1058. https://doi.org/10.1007/s11027-014-9565-4.

Anthony F, Boswijk G, Fowler A. 2003. Chronology stripping as a tool for enhancing the statistical quality of tree-ring chronologies. *Tree-Ring Res* **59**: 53–62.

Aosaar J, Drenkhan T, Adamson K, Aun K, Becker H, et al. 2020. The effect of stump harvesting on tree growth and the infection of root rot in young Norway spruce stands in hemiboreal Estonia. *For Ecol Manage* **475**: 118425. https://doi.org/10.1016/j.foreco.2020. 118425.

Ashraf MI, Bourque CPA, MacLean DA, Erdle T, Meng FR. 2015. Estimation of potential impacts of climate change on growth and yield of temperate tree species. *Mitig Adapt Strateg Glob Chang* **20**: 159–178. https://doi.org/10.1007/s11027-013-9484-9.

Baldwin MP, Ayarzagüena B, Birner T, Butchart N, Butler AH, et al. 2021. Sudden stratospheric warmings. *Rev Geophys* **59**: 1–37. https://doi.org/10.1029/2020RG000708.

Baldwin MP, Gray LJ, Dunkerton TJ, Hamilton K, Haynes PH, et al. 2001. The quasi-biennial oscillation. *Rev Geophys* **39**: 179–229.

Ball WT, Rozanov EV, Alsing J, Marsh DR, Tummon F, Mortlock DJ, Kinnison D, Haigh JD. 2019. The upper stratospheric solar cycle ozone response. *Geophys Res Lett* **46**: 1831–1841. https://doi.org/10.1029/2018GL081501.

Ballaré CL, Cecilia Rousseaux M, Searles PS, Zaller JG, Giordano CV, Matthew Robson T, Caldwell MM, Sala OE, Scopel AL. 2001. Impacts of solar ultraviolet-B radiation on terrestrial ecosystems of Tierra del Fuego (southern Argentina). an overview of recent progress. *J Photochem Photobiol B Biol* **62**: 67–77. https://doi.org/10.1016/S1011-1344(01)00152-X.

Bice D, Montanari A, Vučetić V, Vučetić M. 2012. The influence of regional and global climatic oscillations on Croatian climate. *Int J Climatol* **32**: 1537–1557. https://doi.org/10.1002/joc.2372.

Blackmon ML. 1976. A climatological spectral study of the 500 mb geopotential height of the northern hemisphere. *J Atmos Sci* **33**, 1607–1623. https://doi.org/10.1175/1520-0469(1976)033<1607:ACSSOT>2.0.CO;2.

Blomquist M, Larsson Herrera S, Hofmann J, Beram RC, Cleary M, Rönnberg J. 2020. Size matters but is big always better? Effectiveness of urea and Phlebiopsis gigantea as treatment against Heterobasidion on *Picea abies* stumps of variable size. *For Ecol Manage* **462**: 117998. https://doi.org/10.1016/j.foreco.2020.117998.

Brönnimann S. 2007. Impact of El Niño-Southern oscillation on European climate. *Rev Geophys* **45**, 1–28. https://doi.org/10.1029/2006RG000199.

Brugnara Y, Brönnimann S, Luterbacher J, Rozanov E. 2013. Influence of the sunspot cycle on the Northern Hemisphere wintertime circulation from long upper-air data sets. *Atmos Chem Phys* **13**: 6275–6288. https://doi.org/10.5194/acp-13-6275-2013.

Bunn A, Korpela M, Biondi F, Campelo F, Mérian P, Qeadan F, Zang C, Pucha-Cofrep D, Wernicke J. 2018. *Dendrochronology program library in R. R package version 1.6.8*. Avaiable at https://r-forge.r-project.org/projects/dplr/.

Bunn AG. 2010. Statistical and visual crossdating in R using the dplR library. *Dendrochronologia* **28**: 251–258. https://doi.org/10.1016/j.dendro.2009.12.001.

Bunn AG. 2008. A dendrochronology program library in R (dplR). *Dendrochronologia* **26**: 115–124. https://doi.org/10.1016/j.dendro.2008.01.002.

Cai W, Borlace S, Lengaigne M, van Rensch P, Collins M, et al. 2010. Increasing frequency of extreme El Niño events due to greenhouse warming Wenju. *Nat Clim Chang* **256**: 1–14. https://doi.org/10.1038/NCLIMATE2100.

Carrer M, Urbinati C. 2004. Age-dependent tree-ring growth responses to climate in larix decidua and Pinus cembra. *Ecology* **85**: 730–740.

Cecchini S, Galli M, Nanni T, Ruggiero L. 1996. Solar variability and ring widths in fossil trees. *Nuovo Cim della Soc Ital di Fis C* **19**: 527–536. https://doi.org/10.1007/BF02523768.

Čermák P, Kolář T, Žid T, Trnka M, Rybníček M. 2019. Norway spruce responses to drought forcing in areas affected by forest decline. *For Syst* **28**: e016. https://doi.org/10.5424/fs/2019283-14868.

Černý J, Pokorný R, Vejpustková M, Šrámek V, Bednář P. 2020. Air temperature is the main driving factor of radiation use efficiency and carbon storage of mature Norway spruce stands under global climate change. *Int J Biometeorol* **64**: 1599–1611. https://doi.org/10.1007/s00484-020-01941-w.

Chapanov Y, Gorshkov V. 2019. Solar activity and cosmic ray influence on the climate. *Geomagn Aeron* **59**: 942–949. https://doi.org/10.1134/S0016793219070090.

Chiodo G, Calvo N, Marsh DR, Garcia-Herrera R. 2012. The 11 year solar cycle signal in transient simulations from the whole atmosphere community climate model. *J Geophys Res Atmos* **117**: 1–21. https://doi.org/10.1029/2011JD016393.

Chiodo G, Oehrlein J, Polvani LM, Fyfe JC, Smith AK. 2019. Insignificant influence of the 11-year solar cycle on the North Atlantic oscillation. *Nat Geosci* **12**: 94–99. https://doi.org/10.1038/s41561-018-0293-3.

ČHMÚ. 2022. *Czech Hydrometeorological Institute*. Available at http://portal.chmi.cz/historicka-data/pocasi/uzemni-srazky (accessed 10.1.22).

Chree C. 1913. Some phenomena of sunspots and of terrestrial magnetism at Kew observatory. *Philos Trans R Soc London Ser A* **212**: 75–116. https://doi.org/10.1098/rsta.1913.00030003.

Cook ER, Seager R, Heim Jr RR, Vose RS, Herweijer C, Woodhouse C. 2010. Megadroughts in North America: placing IPCC projections of hydroclimatic change in a long-term palaeoclimate context. *J Quat Sci* **25**: 48–61. https://doi.org/10.1002/jqs.1303.

Cook ER, Shiyatov SG, Mazepa VS, Ecology A, Branch U. 1990. *Methods of dendrochronology applications*. Tree-Ring Laboratory, Lamont-Ooherty Geological Observatory, Columbia University, New York, NY, USA. https://doi.org/10.1007/978-94-015-7879-0.

Coy L, Newman PA, Pawson S, Lait LR. 2017. Dynamics of the disrupted 2015/16 quasi-biennial oscillation. *J. Clim.* **30**: 5661–5674. https://doi.org/10.1175/JCLI-D-16-0663.1.

CRU-UEA. 2023. *North Atlantic Oscillation (NAO) data, Climatic Research Unit, University of East Anglia*. Available at https://crudata.uea.ac.uk/cru/data/nao/index.htm (accessed 11.10.23).

Cukor J, Vacek Z, Linda R, Vacek S, Marada P, Šimůnek V, Havránek F. 2019. Effects of bark stripping on timber production and structure of Norway Spruce forests in relation to climatic factors. *Forests* **10**: 13–17. https://doi.org/10.3390/f10040320.

CZSO – Czech Statistical Office. 2021. *Czech Statistical Office webpage Forestry – 2021*, Available at https://www.czso.cz/csu/czso/home (accessed 10.1.22).

Dasi-Espuig M, Jiang J, Krivova NA, Solanki SK, Unruh YC, Yeo KL . 2016. Reconstruction of spectral solar irradiance since 1700 from simulated magnetograms. *A&A* **590**: 1–13. https://doi.org/10.1051/0004-6361/201527993.

Dobor L, Hlásny T, Rammer W, Zimová S, Barka I, Seidl R. 2020. Is salvage logging effectively dampening bark beetle outbreaks and preserving forest carbon stocks? *J Appl Ecol* **57**: 67–76. https://doi.org/10.1111/1365-2664.13518.

Drews A, Huo W, Matthes K, Kodera K, Kruschke T. 2022. The Sun's role in decadal climate predictability in the North Atlantic. *Atmos Chem Phys* **22**: 7893–7904. https://doi.org/10.5194/acp-22-7893-2022.

Dudok de Wit T, Kopp G, Fröhlich C, Schöll M. 2017. Methodology to create a new total solar irradiance record: making a composite out of multiple data records. *Geophys Res Lett* **44**: 1196–1203. https://doi.org/10.1002/2016GL071866.

Floyd LE, Cook JW, Herring LC, Crane PC. 2002. SUSIM'S 11-year observational record of the solar UV irradiance. *Adv Space Res* **31**: 2111–2120. https://doi.org/10.1016/S0273-1177(03)00148-0.

Floyd L, Rottman G, Deland M, Pap J. 2003. 11 years of solar UV irradiance measurements from UARS. *Eur Space Agency* **535**: 195–203.

Foukal P, Fröhlich C, Spruit H, Wigley TML. 2006. Variations in solar luminosity and their effect on the Earth's climate. *Nature* **443**: 161–166. https://doi.org/10.1038/nature05072.

Fritts HC. 1976. *Tree rings and climate*. Academic Press Inc., New York.

Fritts HC. 1966. Growth-rings of trees: their correlation with climate. *Science* **154**: 973–979. https://doi.org/10.1126/science.154.3752.973.

Gray LJ, Ball W, Misios S. 2017. Solar influences on climate over the Atlantic/European sector. *AIP Conf Proc* **1810**: 020002. https://doi.org/10.1063/1.4975498.

Gray LJ, Beer J, Geller M, Haigh JD, Lockwood M, et al. 2010. Solar influences on climate. *Rev Geophys* **48**: RG4001. https://doi.org/10.1029/2009RG000282.

Halberg F, Cornélissen G, Sothern RB, Czaplicki J, Schwartzkopff O. 2010. Thirty five year climatic cycle in heliogeophysics, psychophysiology, military politics, and economics. *Atmos Ocean Phys* **46**: 40–60. https://doi.org/10.1134/S0001433810070054.

Hall R, Erdélyi R, Hanna E, Jones JM, Scaife AA. 2015. Drivers of North Atlantic Polar Front jet stream variability. *Int J Climatol* **35**: 1697–1720. https://doi.org/10.1002/joc.4121.

Hanewinkel M, Cullmann DA, Schelhaas MJ, Nabuurs GJ, Zimmermann NE. 2013. Climate change may cause severe loss in the economic value of European forest land. *Nat Clim Chang* **3**: 203–207. https://doi.org/10.1038/nclimate1687.

Hartl-Meier C, Zang C, Büntgen U, Esper J, Rothe A, Göttlein A, Dirnböck T, Treydte K. 2018. Uniform climate sensitivity in tree-ring stable isotopes across species and sites in a mid-latitude temperate forest. *Tree Physiol* **35**: 4–15. https://doi.org/10.1093/treephys/tpu096.

Hathaway DH. 2015. The solar cycle. *Living Rev Sol Phys* **12**: 83. https://doi.org/10.1007/lrsp-2015-4.

Helama S, Meriläinen J, Tuomenvirta H. 2009. Multicentennial megadrought in northern Europe coincided with a global El Niño–Southern Oscillation drought pattern during the Medieval Climate Anomaly. *Geology*: **37**: 175–178. https://doi.org/10.1130/G25329A.1.

Hlásny T, Barcza Z, Barka I, Merganičová K, Sedmák R, Kern A, Pajtík J, Balázs B, Fabrika M, Churkina G. 2014. Future carbon cycle in mountain spruce forests of Central Europe: modelling framework and ecological inferences. *For Ecol Manage* **328**: 55–68. https://doi.org/10.1016/j.foreco.2014.04.038.

Hlásny T, Barka I, Roessiger J, Kulla L, Trombik J, Sarvašová Z, Bucha T, Kovalčík M, Čihák T. 2017. Conversion of Norway spruce forests in the face of climate change: a case study in Central Europe. *Eur J For Res* **136**: 1013–1028. https://doi.org/10.1007/s10342-017-1028-5.

Hlásny T, König L, Krokene P, Lindner M, Montagné-Huck C, et al. 2021a. Bark beetle outbreaks in europe: state of knowledge and ways forward for management. *Curr For Rep* **7**: 138–165. https://doi.org/10.1007/s40725-021-00142-x.

Hlásny T, Turčáni M. 2013. Persisting bark beetle outbreak indicates the unsustainability of secondary Norway spruce forests: case study from Central Europe. *Ann For Sci* **70**: 481–491. https://doi.org/10.1007/s13595-013-0279-7.

Hlásny T, Zimová S, Merganičová K, Štěpánek P, Modlinger R, Turčáni M. 2021b. Devastating outbreak of bark beetles in the Czech Republic: drivers, impacts, and management implications. *For Ecol Manage* **490**: 119075. https://doi.org/10.1016/j.foreco.2021.119075.

Holuša J, Lubojacký J, Čurn V, Tonka T, Lukášová K, Horák J. 2018. Combined effects of drought stress and Armillaria infection on tree mortality in Norway spruce plantations. *For Ecol Manage* **427**: 434–445. https://doi.org/10.1016/j.foreco.2018.01.031.

Jandl R. 2020. Climate-induced challenges of Norway spruce in Northern Austria. *Trees For People* **1**: 100008. https://doi.org/10.1016/j.tfp.2020.100008.

Jones PD, Jonsson T, Wheeler D. 1997. Extension to the North Atlantic Oscillation using early instrumental pressure observations from gibraltar and south-west Iceland. *Int J Climatol* **17**: 1433–1450. https://doi.org/10.1002/(SICI)1097-0088(19971115)17:13<1433::AID-JOC203>3.0.CO;2-P.

Kärhä K, Anttonen T, Poikela A, Palander T, Laurén A, Peltola H, Nuutinen Y. 2018. Evaluation of salvage logging productivity and costs in windthrown Norway spruce-dominated forests. *Forests* **9**: 280. https://doi.org/10.3390/f9050280.

Kasatkina EA, Shumilov OI, Timonen M. 2019. Solar activity imprints in tree ring-data from northwestern Russia. *J Atmos Solar Terr Phys* **193**: 105075. https://doi.org/10.1016/j.jastp.2019.105075.

Kjellström E, Thejll P, Rummukainen M, Christensen JH, Boberg F, Christensen OB, Maule CF. 2013. Emerging regional climate change signals for Europe under varying large-scale circulation conditions. *Clim Res* **56**: 103–119. https://doi.org/10.3354/cr01146.

Kolář T, Čermák P, Trnka M, Žid T, Rybníček M . 2017. Temporal changes in the climate sensitivity of Norway spruce and European beech along an elevation gradient in Central Europe. *Agric For Meteorol* **239**: 24–33. https://doi.org/10.1016/j.agrformet.2017. 02.028.

Komitov B. 2021. The European beech annual tree ring widths time series, solar–climatic relationships and solar dynamo regime changes. *Atmosphere (Basel)* **12**: 1–26. https://doi.org/10.3390/atmos12070829.

Kopáček J, Cudlín P, Fluksová H, Kaňa J, Picek T, Šantrůčková H, Svoboda M, Vaněk D. 2015. Dynamics and composition of litterfall in an unmanaged Norway spruce. *Boreal Environ Res* **6095**: 305–323.

Kopp G. 2021. Greg Kopp's TSI Page. *TSI Clim. Data Rec.* Available at https://spot.colorado.edu/~koppg/TSI/ (accessed 2.4.21).

Kopp G, Krivova N, Wu CJ, Lean J. 2016. The impact of the revised sunspot record on solar irradiance reconstructions. *Sol. Phys.* **291**: 2951–2965. https://doi.org/10.1007/s11207-016-0853-x.

Kopp G, Lean JL. 2011. A new, lower value of total solar irradiance: evidence and climate significance. *Geophys Res Lett* **38**: 1–7. https://doi.org/10.1029/2010GL045777.

Köppen W. 1936. *Das Geographische System der Klimate, Handbuch der Klimatologie*. Gebrüder Borntraeger, Berlin.

Kotsias G, Lolis CJ, Hatzianastassiou N, Levizzani V, Bartzokas A. 2020. On the connection between large-scale atmospheric circulation and winter GPCP precipitation over the Mediterranean region for the period 1980–2017. *Atmos. Res.* **233**: 104714. https://doi.org/10.1016/j.atmosres.2019.104714.

Krisans O, Saleniece R, Rust S, Elferts D, Kapostins R, Jansons A, Matisons R. 2020. Effect of bark-stripping on mechanical stability of Norway spruce. *Forests* **11**: 357. https://doi.org/10.3390/f11030357.

Kukumägi M, Ostonen I, Uri V, Helmisaari HS, Kanal A, Kull O, Lõhmus K. 2017. Variation of soil respiration and its components in hemiboreal Norway spruce stands of different ages. *Plant Soil* **414**: 265–280. https://doi.org/10.1007/s11104-016-3133-5.

Kundzewicz ZW, Radziejewski M, Pińskwar I. 2006. Precipitation extremes in the changing climate of Europe. *Clim Res* **31**: 51–58. https://doi.org/10.3354/cr031051.

Labitzke K. 2005. On the solar cycle-QBO relationship: a summary. *J Atmos Solar Terr Phys* **67**: 45–54. https://doi.org/10.1016/j.jastp.2004.07.016.

Laken BA, Čalogović J. 2013. Composite analysis with monte carlo methods: an example with cosmic rays and clouds. *J Space Weather Space Clim* **3**: 1–13. https://doi.org/10.1051/swsc/2013051.

Larsson LA. 2013. *Cybis Elektronik & Data AB*. Available at http://www.cybis.se/ (accessed 6.20.19).

Laurenz L, Lüdecke HJ, Lüning S. 2019. Influence of solar activity changes on European rainfall. *J Atmos Solar Terr Phys* **185**: 29–42. https://doi.org/10.1016/j.jastp.2019.01.012.

Leonelli G, Coppola A, Salvatore MC, Baroni C, Battipaglia G, et al. 2017. Climate signals in a multispecies tree-ring network from central and southern Italy and reconstruction of the late summer temperatures since the early 1700s. *Clim Past* **13**: 1451–1471. https://doi.org/10.5194/cp-13-1451-2017.

Lockwood M, Owens MJ, Barnard L. 2014. Centennial variations in sunspot number, open solar flux, and streamer belt width: 2. Comparison with the geomagnetic data. *J Geophys Res Space Phys*, **119**: 5183–5192. https://doi.org/10.1002/2014JA019972.

Lüdecke HJ, Cina R, Dammschneider HJ, Lüning S. 2020. Decadal and multidecadal natural variability in European temperature. *J Atmos Solar Terr Phys* **205**: 105294. https://doi.org/10.1016/j.jastp.2020.105294.

Ma H, Chen H, Gray L, Zhou L, Li X, Wang R, Zhu S. 2018. Changing response of the North Atlantic/European winter climate to the 11 year solar cycle. *Environ Res Lett* **13**: 034007. https://doi.org/10.1088/1748-9326/aa9e94.

Madronich S. 1993. The atmosphere and UV-B radiation at ground level. In: *Environmental UV photobiology*, Young AR, Moan J, Björn LO, Nultsch W (Eds.), Springer: Boston, MA, pp. 1–39. https://doi.org/10.1007/978-1-4899-2406-3_1.

MAF. 2018. *Report about forest and forestry conditions in the Czech Republic 2017*, The Ministry of Agriculture of the Czech Republic.

MAF. 2020. *Report about forest and forestry conditions in the Czech Republic 2019*, The Ministry of Agriculture of the Czech Republic, Prague.

MAF. 2021. *Report about forest and forestry conditions in the Czech Republic 2021*, The Ministry of Agriculture of the Czech Republic, Prague.

Marini L, Lindelöw Å, Jönsson AM, Wulff S, Schroeder LM. 2013. Population dynamics of the spruce bark beetle: a long-term study. *Oikos* **122**: 1768–1776. https://doi.org/10.1111/j.1600-0706.2013.00431.x.

Marini L, Økland B, Jönsson AM, Bentz B, Carroll A, et al. 2017. Climate drivers of bark beetle outbreak dynamics in Norway spruce forests. *Ecography (Cop.)* **40**: 1426–1435. https://doi.org/10.1111/ecog.02769.

Matějka K, Vacek S, Podrázský V. 2010. Development of forest soils in the Krkonoše Mts. in the period 1980–2009. *J For Sci* **56**: 485–504.

Materna J. 1989. Air pollution and forestry in Czechoslovakia. *Environ Monit Assessment* **12**: 227–239.

Matveev SM, Chendev YG, Lupo AR, Hubbart JA, Timashchuk DA. 2017. Climatic changes in the east-european forest-steppe and effects on scots pine productivity. *Pure Appl Geophys* **174**: 427–443. https://doi.org/10.1007/s00024-016-1420-y.

Maycock AC, Matthes K, Tegtmeier S, Schmidt H, Thiéblemont R, et al. 2018. The representation of solar cycle signals in stratospheric ozone – part 2: analysis of global models. *Atmos Chem Phys* **18**: 11323–11343. https://doi.org/10.5194/acp-18-11323-2018.

Maycock AC, Matthes K, Tegtmeier S, Thiéblemont R, Hood L. 2016. The representation of solar cycle signals in stratospheric ozone – part 1: a comparison of recently updated satellite observations. *Atmos Chem Phys* **16**: 10021–10043. https://doi.org/10.5194/acp-16-10021-2016.

Mezei P, Potterf M, Škvarenina J, Rasmussen JG, Jakuš R. 2019. Potential solar radiation as a driver for bark beetle infestation on a landscape scale. *Forests* **10**: 1–12. https://doi.org/10.3390/f10070604.

Mikol M, Janda P, Spînu AP, Cat I. 2020. moderate- to high-severity disturbances shaped the structure of primary *Picea abies* [L.] Karst. Forest in the Southern Carpathians. *Forests* **11**: 1315. https://doi.org/10.3390/f11121315.

Mikulenka P, Prokůpková A, Vacek Z, Vacek S, Bulušek D, Simon J, Šimůnek V, Hájek V. 2020. Effect of climate and air pollution on radial growth of mixed forests: *Abies alba Mill* vs. *Picea abies* (L.) Karst. *Cent. Eur. For. J.* **66**: 23–36. https://doi.org/10.2478/forj-2019-0026.

Mitchell SJ. 2013. Wind as a natural disturbance agent in forests: a synthesis. *Forestry* **86**: 147–157. https://doi.org/10.1093/forestry/cps058.

Nascimbene J, Thor G, Nimis PL. 2013. Effects of forest management on epiphytic lichens in temperate deciduous forests of Europe – a review. *For Ecol Manage* **298**: 27–38. https://doi.org/10.1016/j.foreco.2013.03.008.

Netherer S, Panassiti B, Pennerstorfer J, Matthews B. 2019. Acute drought is an important driver of bark beetle infestation in Austrian Norway spruce stands. *Front For Glob Chang* **2**: 1–21. https://doi.org/10.3389/ffgc.2019.00039.

Noce S, Collalti A, Valentini R, Santini M. 2016. Hot spot maps of forest presence in the Mediterranean basin. *IForest* **9**: 766–774. https://doi.org/10.3832/ifor1802-009.

Nováková MH, Edwards-Jonášová M. 2015. Restoration of central-european mountain norway spruce forest 15 years after natural and anthropogenic disturbance. *For Ecol Manage* **344**: 120–130. https://doi.org/10.1016/j.foreco.2015.02.010.

Nownes AJ. 2012. Methodological Notes, Czech Statistical Office. In: *Total Lobbying*, Cambridge University Press, Cambridge, UK, pp. 225–232. https://doi.org/10.1017/CBO9780511840395.010.

Økland B, Berryman A. 2004. Resource dynamic plays a key role in regional fluctuations of the spruce bark beetles Ips typographus. *Agric For Entomol* **6**: 141–146. https://doi.org/10.1111/j.1461-9555.2004.00214.x.

Peterson CJ, Leach AD. 2008. Salvage logging after windthrow alters microsite diversity, abundance and environment, but not vegetation. *Forestry* **81**: 361–376. https://doi.org/10.1093/forestry/cpn007.

Piovesan G, Schirone B. 2000. Winter North Atlantic oscillation effects on the tree rings of the Italian beech (*Fagus sylvatica* L.). *Int J Biometeorol* **44**: 121–127. https://doi.org/10.1007/s004840000055.

Piri T. 1996. The spreading of the S type of Heterobasidion annosum from Norway spruce stumps to the subsequent tree stand. *Eur J For Pathol* **26**: 193–204. https://doi.org/10.1111/j.1439-0329.1996.tb00839.x.

Remeš J, Bílek L, Novák J, Vacek Z, Vacek S, Putalová T, Koubek L. 2015. Diameter increment of beech in relation to social position of trees, climate characteristics and thinning intensity. *J For Sci* **61**: 456–464. https://doi.org/10.17221/75/2015-JFS.

Remeš J, Pulkrab K, Bílek L, Podrázský V. 2020. Economic and production effect of tree species change as a result of adaptation to climate change. *Forests* **11**: 431. https://doi.org/10.3390/F11040431.

Rigozo NR, Nordemann DJR, Echer E, Zanandrea A, Gonzalez WD. 2002. Solar variability effects studied by tree-ring data wavelet analysis. *Adv Space Res* **29**: 1985–1988. https://doi.org/10.1016/S0273-1177(02)00245-4.

Rigozo NR, Nordemann DJR, Souza Echer MP, Echer E, da Silva HE, Prestes A, Guarnieri FL. 2007. Solar activity imprints in tree ring width from Chile (1610–1991). *J Atmos Solar Terr Phys* **69**: 1049–1056. https://doi.org/10.1016/j.jastp.2007.03.010.

Rimbu N, Lohmann G, Ionita M, Czymzik M, Brauer A. 2021. Interannual to millennial-scale variability of River Ammer floods and its relationship with solar forcing. *Int J Climatol* **41**: E644–E655. https://doi.org/10.1002/joc.6715.

Rinntech. 2010. *TSAP-WIN: time series analysis and presentation for dendrochronology and related applications*.Available at http://www.rinntech.com (accessed 5.2.22).

Rybníček M, Čermák P, Žid T, Kolář T. 2012. Growth responses of *Picea abies* to climate in the central part of the Českomoravská Upland (Czech Republic). *Dendrobiology* **68**: 21–30.

Rybníček M, Čermák P, Žid T, Kolář T. 2010. Radial growth and health condition of Norway spruce (*Picea abies* (L.) Karst.) stands in relation to climate (Silesian Beskids, Czech Republic). *Geochronometria* **36**: 9–16. https://doi.org/10.2478/v10003-010-0017-1.

Salby ML, Shea DJ . 1991. Correlations between solar activity and the atmosphere: An unphysical explanation. *J Geophys Res Atmos* **96**: 22579–22595. https://doi.org/10.1029/91JD02530.

Scafetta N. 2012. Multi-scale harmonic model for solar and climate cyclical variation throughout the Holocene based on Jupiter-Saturn tidal frequencies plus the 11-year solar dynamo cycle. *J Atmos Solar-Terr Phys* **80**: 296–311. https://doi.org/10.1016/j.jastp.2012.02.016.

Scaife AA, Ineson S, Knight JR, Gray L, Kodera K, Smith DM. 2013. A mechanism for lagged North Atlantic climate response to solar variability. *Geophys Res Lett* **40**: 434–439. https://doi.org/10.1002/grl.50099.

Schroeder LM, Lindelöw Å. 2002. Attacks on living spruce trees by the bark beetle ips typographus (Col. Scolytidae) following a storm-felling: A comparison between stands with and without removal of wind-felled trees. *Agric For Entomol* **4**: 47–56. https://doi.org/10.1046/j.1461-9563.2002.00122.x.

Seidl R, Müller J, Hothorn T, Bässler C, Heurich M, Kautz M. 2016. Small beetle, large-scale drivers: How regional and landscape factors affect outbreaks of the European spruce bark beetle. *J Appl Ecol* **53**: 530–540. https://doi.org/10.1111/1365-2664.12540.

Seidl R, Rammer W, Lasch P, Badeck FW, Lexer MJ. 2008. Does conversion of even-aged, secondary coniferous forests affect carbon sequestration? A simulation study under changing environmental conditions. *Silva Fenn.* **42**: 369–386. https://doi.org/10.14214/sf.243.

Shi F, Li J, Wilson RJS. 2014. A tree-ring reconstruction of the South Asian summer monsoon index over the past millennium. *Sci. Rep.* **4**: 1–8. https://doi.org/10.1038/srep06739.

Shumilov OI, Kasatkina EA, Mielikainen K, Timonen M, Kanatjev AG. 2011. Palaeovolcanos, Solar activity and pine tree-rings from the Kola Peninsula (northwestern Russia) over the last 560 years Palaeovolcanos. *Int J Environ Res* **5**: 855–864. https://doi.org/10.22059/IJER.2011.443.

Šimůnek V, Hájek V, Prokůpková A, Gallo J. 2021a. Finding an imprint of solar and climatic cycles in tree rings of European beech (*Fagus sylvatica* L.). *J For Sci* **67**: 409–419. https://doi.org/10.17221/94/2020-JFS.

Šimůnek V, Sharma RP, Vacek Z, Vacek S, Hůnová I. 2020a. Sunspot area as unexplored trend inside radial growth of European beech in Krkonoše Mountains: a forest science from different perspective. *Eur J For Res* **139**: 999–1013. https://doi.org/10.1007/s10342-020-01302-7.

Šimůnek V, Vacek Z, Vacek S. 2020b. Solar cycles in salvage logging: National data from the Czech Republic confirm significant correlation. *Forests* **11**: 1–22. https://doi.org/10.3390/f11090973.

Šimůnek V, Vacek Z, Vacek S, Králíček I, Vančura K. 2019. Growth variability of European beech (*Fagus sylvatica* L) natural forests: Dendroclimatic study from Krkonoše National Park. *Cent Eur For J* **65**: 92–102. https://doi.org/10.2478/forj-2019-0010.

Šimůnek V, Vacek Z, Vacek S, Ripullone F, Hájek V, D'andrea G. 2021b. Tree rings of european beech (*Fagus sylvatica* L.) indicate the relationship with solar cycles during climate change in central and southern europe. *Forests* **12**: 1–22. https://doi.org/10.3390/f12030259.

Speer JH. 2010. *Fundamentals of tree-ring research. Geoarchaeology*. University of Arizona Press, Tuscon, ISBN 0816526850. https://doi.org/10.1002/gea.20357.

Spiecker H. 2003. Silvicultural management in maintaining biodiversity and resistance of forests in Europe – Temperate zone. *J Environ Manage* **67**: 55–65. https://doi.org/10.1016/S0301-4797(02)00188-3.

Spiegl TC, Langematz U, Pohlmann H, Kröger J. 2023. A critical evaluation of decadal solar cycle imprints in the MiKlip historical ensemble simulations. *Weather Clim Dyn* **4**: 789–807. https://doi.org/10.5194/wcd-4-789-2023.

St. George, S. 2014. An overview of tree-ring width records across the Northern Hemisphere. *Quat. Sci. Rev.* **95**: 132–150. https://doi.org/10.1016/j.quascirev.2014.04.029.

StatSoft. 2013. *Statistica electronic manual*. Tulsa, OK, USA. http://www.statsoft.com/textbook.

Steirou E, Gerlitz L, Apel H, Merz B. 2017. Links between large-scale circulation patterns and streamflow in Central Europe: a review. *J Hydrol* **549**: 484–500. https://doi.org/10.1016/j.jhydrol.2017.04.003.

Surový P, Ribeiro NA, de Evora U, Pereira JS, Superior I, Lisbon DA. 2008. Influence of solar activity cycles on cork growth–a hypothesis. In: *Proceedings of the 19th National Solar Physics Meeting*. Dorotovič I (Ed), Hurbanovo, SÚH, Papradno, pp. 67–72.

Tartaglione N, Toniazzo T, Orsolini Y, Otterå OH. 2020. Impact of solar irradiance and geomagnetic activity on polar NOx, ozone and temperature in WACCM simulations. *J Atmos Sol-Terr Phys* **209**: 105398. https://doi.org/10.1016/j.jastp.2020.105398.

Tatli H, Menteş ŞS. 2019. Detrended cross-correlation patterns between North Atlantic oscillation and precipitation. *Theor Appl Climatol* **138**: 387–397. https://doi.org/10.1007/s00704-019-02827-7.

Team R Core. 2022. *A language and environment for statistical computing*. R Foundation for Statistical Computing, Vienna, Austria, Available at https://www.r-project.org/ (accessed 8.8.22).

Thiele JC, Nuske RS, Ahrends B, Panferov O, Albert M, Staupendahl K, Junghans U, Jansen M, Saborowski J. 2017. Climate change impact assessment–A simulation experiment with Norway spruce for a forest district in Central Europe. *Ecol Modell* **346**: 30–47. https://doi.org/10.1016/j.ecolmodel.2016.11.013.

Toth D, Maitah M, Maitah K, Jarolínová V. 2020. The impacts of calamity logging on the development of spruce wood prices in czech forestry. *Forests* **11**: 1–13. https://doi.org/10.3390/f11030283.

Trouet V, Esper J, Graham NE, Baker A, Scourse JD, Frank DC. 2009. Persistent positive North Atlantic oscillation mode dominated the medieval climate anomaly. *Science* **324**: 78–80. https://doi.org/10.1126/science.1166349.

Tsanis I, Tapoglou E. 2019. Winter North Atlantic Oscillation impact on European precipitation and drought under climate change. *Theor Appl Climatol* **135**: 323–330. https://doi.org/10.1007/s00704-018-2379-7.

Tsiropoula G. 2003. Signatures of solar activity variability in meteorological parameters. *J Atmos Solar-Terr Phys* **65**: 469–482. https://doi.org/10.1016/S1364-6826(02)00295-X.

Tumajer J, Altman J, Štěpánek P, Treml V, Doležal J, Cienciala E. 2017. Increasing moisture limitation of Norway spruce in Central Europe revealed by forward modelling of tree growth in tree-ring network. *Agric For Meteorol* **247**: 56–64. https://doi.org/10.1016/j.agrformet.2017.07.015.

Turčáni M, Hlásny T. 2007. Spatial distribution of four spruce bark beetles in north-western Slovakia. *J For Sci* **53**: 45–52. https://doi.org/10.17221/2157-jfs.

Uğur B, Feriha Y. 2017. Forecasting risky years for forest fires depending on sunspot cycle. *J. For. Res.* **4**: 133–142.

Usoskin IG, Gallet Y, Lopes F, Kovaltsov GA, Hulot G. 2016. Solar activity during the Holocene: the Hallstatt cycle and its consequence for grand minima and maxima. *A&A* **587**: 1–10. https://doi.org/10.1051/0004-6361/201527295.

Vacchiano G, Derose RJ, Shaw JD, Svoboda M, Motta R. 2013. A density management diagram for Norway spruce in the temperate European montane region. *Eur J For Res* **132**: 535–549. https://doi.org/10.1007/s10342-013-0694-1.

Vacek S, Hejcmanová P, Hejcman M, Vacek Z. 2013. Growth, healthy status and seed production of differently aged allochtonous and autochtonous *Pinus mugo* stands in the Giant Mts. over 30 years. *Eur J For Res* **132**: 801–813. https://doi.org/10.1007/s10342-013-0721-2.

Vacek S, Hůnová I, Vacek Z, Hejcmanová P, Podrázský V, Král J, Putalová T, Moser WK. 2015a. Effects of air pollution and climatic factors on Norway spruce forests in the Orlické hory Mts. (Czech Republic), 1979–2014. *Eur J For Res* **134**: 1127–1142. https://doi.org/10.1007/s10342-015-0915-x.

Vacek S, Prokůpková A, Vacek Z, Bulušek D, Simunek V, Králícek I, Prausová R, Hájek V. 2019. Growth response of mixed beech forests to climate change, various management and game pressure in Central Europe. *J For Sci* **65**: 331–345. https://doi.org/10.17221/82/2019-JFS.

Vacek S, Vacek Z, Bílek L, Hejcmanová P, Štícha V, Remeš J. 2015b. The dynamics and structure of dead wood in natural spruce-beech forest stand – a 40 year case study in the Krkonoše national park. *Dendrobiology* **73**: 21–32. https://doi.org/10.12657/denbio.073.003.

Vacek S, Zingari PC, Jeník J, Simon J, Smejkal J, Vančura K. 2003. *Mountain forests of the Czech Republic*. Ministry of agriculture of the Czech Republic, Prague.

Vacek Z, Cukor J, Linda R, Vacek S, Šimůnek V, Brichta J, Gallo J, Prokůpková A. 2020. Bark stripping, the crucial factor affecting stem rot development and timber production of Norway spruce forests in Central Europe. *For Ecol Manage* **474**: 118360. https://doi.org/10.1016/j.foreco.2020.118360.

Vacek Z, Prokůpková A, Vacek S, Bulušek D, ŠimůnekV, Hájek V, Králíček I. 2021. Mixed vs. monospecific mountain forests in response to climate change: structural and growth perspectives of Norway spruce and European beech. *For Ecol Manage* **488**: 119019. https://doi.org/10.1016/j.foreco.2021. 119019.

Vacek Z, Vacek S, Cukor J. 2023. European forests under global climate change: review of tree growth processes, crises and management strategies. *J Environ Manage* **332**: 117353. https://doi.org/10.1016/j.jenvman.2023.117353.

Vicente-Serrano SM, López-Moreno JI, Lorenzo-Lacruz J, El Kenawy A, Azorin-Molina C, Morán-Tejeda E, Pasho E, Zabalza J, Beguería S, Angulo-Martínez M. 2011. The NAO Impact on droughts in the mediterranean region BT. In: *Hydrological, socioeconomic and ecological impacts of the north atlantic oscillation in the mediterranean region*. Vicente-Serrano SM, Trigo RM (Eds), Springer Netherlands, Dordrecht, pp. 23–40. https://doi.org/10.1007/978-94-007-1372-7_3.

Viewegh J, Kusbach A, Mikeska M. 2003. Czech forest ecosystem classification. *J For Sci* **49**: 85–93.

Wang X, Zhang Q-B. 2011. Evidence of solar signals in tree rings of Smith fir from Sygera Mountain in southeast Tibet. *J Atmos Sol-Terr Phys*. **73**: 1959–1966. https://doi.org/10.1016/j.jastp.2011.06.001.

Wang Y-M, Lean JL, Sheeley Jr NR. 2005. Modeling the Sun's magnetic field and irradiance since 1713. *Astrophys J* **625**: 522–538. https://doi.org/10.1086/429689.

Wibig J, Piotrowski P. 2018. Impact of the air temperature and atmospheric circulation on extreme precipitation in Poland. *Int J Climatol* **38**: 4533–4549. https://doi.org/10.1002/joc.5685.

Wu CJ, Krivova NA, Solanki SK, Usoskin IG. 2018. Solar total and spectral irradiance reconstruction over the last 9000 years. *A&A* **620**: 1–12. https://doi.org/10.1051/0004-6361/201832956.

Yao Y, Luo DH. 2014. Relationship between zonal position of the North Atlantic Oscillation and Euro-Atlantic blocking events and its possible effect on the weather over Europe. *Sci China Earth Sci* **57**: 2628–2636. https://doi.org/10.1007/s11430-014-4949-6.

Ye A, Zhu Z, Zhang R, Xiao Z, Zhou L. 2023. Influence of solar forcing on multidecadal variability in the Atlantic meridional overturning circulation (AMOC). *Front Earth Sci* **11**: 1–16. https://doi.org/10.3389/feart.2023.1165386.

Yeo KL, Krivova NA, Solanki SK. 2017. EMPIRE: a robust empirical reconstruction of solar irradiance variability. *J Geophys Res Space Phys* **122**: 3888–3914. https://doi.org/10.1002/2016JA023733.

Zahradník P, Zahradníková M. 2019. Salvage felling in the Czech Republic's forests during the last twenty years. *Cent Eur For J* **65**: 12–20. https://doi.org/10.2478/forj-2019-0008.

Zang C, Buras A, Cecile J, Mudelsee M, Schulz M, Pucha-cofrep D. 2018. *Package "dplR" R Dendrochronology Program Library in R Version*. Available at https://r-forge.r-project.org/projects/dplr/ (accessed 6.25.20).

Cite this article as: Šimůnek V, Vacek Z, Vacek S, Švanda M, Hájek V, et al. 2024. Norway spruce forest management in the Czech Republic is linked to the solar cycle under conditions of climate change – from tree rings to salvage harvesting. *J. Space Weather Space Clim.* **14**, 37. https://doi.org/10.1051/swsc/2024030.